

Analysis of Lidar Data for Improved Flood Risk Mapping:

Enhanced Lidar Point Cloud Classification and Product Development



Nova Scotia Community College
Applied Geomatics Research Group
NSCC, Middleton, NS
Tel. 902 825 5475
Email: timothy.webster@nsc.ca

Colin MacDonald
Director, Geographic Information Services
ICT Services, Internal Services Department
Government of Nova Scotia
5161 George St.
Halifax, NS B3J 2Y1
March 31st, 2022

How to cite this work and report:

NSCC Applied Geomatics Research Group. 2022. Analysis of Lidar Data for Improved Flood Risk Mapping: Enhanced Lidar Point Cloud Classification and Product Development. Technical report, Applied Geomatics Research Group, NSCC Middleton, NS.

Copyright and Acknowledgement

The Applied Geomatics Research Group of the Nova Scotia Community College maintains full ownership of all data collected by equipment owned by NSCC and agrees to provide the end user who commissions the data collection a license to use the data for the purpose they were collected for upon written consent by AGRG-NSCC. The end user may make unlimited copies of the data for internal use; derive products from the data, release graphics and hardcopy with the copyright acknowledgement of **“Data acquired and processed by the Applied Geomatics Research Group, NSCC”**. Data acquired using this technology and the intellectual property (IP) associated with processing these data are owned by AGRG/NSCC and data will not be shared without permission of AGRG/NSCC.

Executive Summary

The following report is one of two produced by the Applied Geomatics Research Group focused on the analysis of lidar data for improved flood risk mapping. This report details how enhanced lidar point cloud classification and product development can improve model accuracies and provide critical data.

Raw lidar data obtained by the Province of Nova Scotia were used to classify buildings in a 4 km² area within the Gaspereau River – Black River watershed. Products derived from the classified lidar included a digital elevation model with buildings, building footprints containing elevation information, and surface roughness layers. An accuracy assessment was conducted by performing spatial joins on the lidar-derived and provincial building footprint layers. Orthoimagery was also used to assess the quality of the building footprints. The automated routine identified 173 buildings within the study area, 18 of which were not present in the provincial database. 16 buildings out of the 172 identified in the provincial building footprint layer were not present in the lidar-derived footprints, however, it was possible to explain each instance of potential misclassification through reinspection in a lidar processing software. The lidar classification was negatively impacted by insufficient point density, partial or complete occlusion, and building size. Additional limitations included steep roof shapes, greenhouses, inaccurate ground classification, and dense vegetation with a uniform height. Overall, the lidar classification and subsequent building footprint generation provided an accurate and time-effective method of updating the current provincial repository of buildings. The location, size, and elevation of buildings could be used to create more robust hydrodynamic models and subsequently improve flood risk management strategies.

Lidar-derived elevation models and intensity images were used to create a land cover classification layer that included vegetated and non-vegetated fields, buildings, unpaved roads, water, and impervious surfaces, hardwood, and softwood classes. The support vector machine (SVM) supervised classification was able to produce a primarily accurate land classification within the study area, however, limitations were identified with the accuracy of the water, unpaved roads, and non-vegetated field classes.

The results of this project demonstrate how existing data assets can be used to generate valuable products for use in flood mapping endeavours. These products can substantially improve the accuracy of flood risk maps, help the province understand the impacts of dealing with existing structures in at risk areas, and develop recommendations on how to improve the Statement of Provincial Interest on Flood Risk Areas.

Table of Contents

Executive Summary.....	iii
Table of Figures.....	vi
List of Tables.....	viii
1 Introduction.....	1
1.1 Project Background.....	1
1.2 Study Area Description.....	3
2 Methods.....	5
2.1 Building Classification.....	5
2.1.1 Lidar Point Classification.....	5
2.1.2 Building Footprints.....	6
2.2 Surface Roughness.....	7
2.3 Land Cover Classification.....	8
3 Results.....	11
3.1 Building Classification.....	11
3.1.1 Lidar Point Classification.....	11
3.1.2 Building Footprints.....	13
3.1.3 Processing Time.....	15
3.2 Surface Roughness.....	16
3.3 Land Cover Classification.....	20
3.3.1 Classifier Training.....	20
3.3.2 Accuracy Assessment.....	22
4 Discussion.....	24
4.1 Building Classification.....	24
4.1.1 Lidar Point Classification.....	24

4.1.2	Building Footprints	34
4.1.3	Province-Wide Effort Estimation.....	40
4.2	Land Cover Classification	41
4.2.1	Classifier Training	41
4.2.2	Expanded Assessment Area	41
4.3	Recommendations.....	42
4.3.1	Impervious Surface Layer	42
4.3.2	Improved Roughness Layers for Modelling Flow	43
4.3.3	Improved Floodplain Prediction.....	43
5	Conclusion	44
6	References.....	46
7	Acknowledgements	47
8	Appendix	48

Table of Figures

Figure 1. Maps of the study area	4
Figure 2. A comparison of potential lidar products to use as inputs to the SVM classifier. A: canopy height model (CHM); B: digital elevation model (DEM); C: digital surface model (DSM); and D: point return intensity (INT).	9
Figure 3. An RGB composite orthophoto clipped to the classification training area.	10
Figure 4. A roughness raster derived from the absolute value of the curvature of the DEM.	10
Figure 2. Result of automated building classification	12
Figure 3. A digital elevation model of the study area	14
Figure 4. A map displaying building footprints	15
Figure 5. A surface roughness map generated from lidar ground returns for the full extent of the study area (A) and in a single 1 km ² tile (B).	17
Figure 6. A map that represents the height of low vegetation above the ground class for the full extent of the study area (A) and in a single 1 km ² tile (B).	18
Figure 7. A map that represents the height of medium vegetation above the ground class for the full extent of the study area (A) and in a single 1 km ² tile (B).	19
Figure 11. Results of four SVM classifiers, using different inputs and training data. A: CHM, DEM, and INT; B: Only CHM and INT; C: CHM, INT, and roughness; and D: CHM and INT with new training sites and distinction between soft and hardwood trees.	21
Figure 12. Two of the composites investigated for use with the SVM classifier. Note the colour change at the edges of B resulting from the inclusion of the DEM. A: Composite of the CHM and INT rasters; and B: Composite of the CHM, DEM, and INT rasters.	22
Figure 8. A comparison of a building footprint identified by the province with the 2015 orthoimagery used to digitize it.	25
Figure 9. A cross-section of a building as identified by the province but not visible in the point cloud. The location of the cross-section (B) is symbolized by a yellow line (A). Provincial building footprints are symbolized with a white polygon (A).	25
Figure 10. A cross-section of a building that was excluded from the automated building classification due to sparse lidar points. The location of the cross-section (B) is symbolized by a yellow line (A). Provincial building footprints are symbolized with a white polygon (A).	26
Figure 11. A cross-section of a building left unclassified by the automated routine due to partial occlusion of the roof. The location of the cross-section is symbolized by a yellow line (A) and the probable	

location of building points is outlined in red (B). Provincial building footprints are symbolized with a white polygon (A)..... 27

Figure 12. A cross-section of a building that was too small to be identified by the classification routine. The location of the cross-section is symbolized by a yellow line (A) and probable building points are circled in red (B). Provincial building footprints are symbolized with a white polygon (A). ... 28

Figure 13. A cross-section of a tree after the automated building classification was conducted with a Very Strict parameter (A) and a Strict parameter (B). 29

Figure 14. A cross-section of a church. The location of the cross-section (B) is symbolized by a yellow line (A). The location of the church steeple is circled in white (A). 30

Figure 15. A cross-section of a greenhouse that failed to be accurately classified by the automated routine. The location of the cross-section (B) is symbolized by a yellow line (A). 31

Figure 16. A cross-section of a building that was not entirely identified by the automated classification routine due to erroneous ground points underneath the building points. The location of the cross-section is symbolized by a yellow line (A) and ground points are circled in red (B). 32

Figure 17. Maps showing the location of a group of misclassified building points in comparison to 2015 orthoimagery. 33

Figure 18. A cross-section of dense vegetation misclassified as a building by the automated routine. The location of the cross-section (B) is symbolized by a yellow line (A). 33

Figure 19. Maps showing a comparison between 2015 orthoimagery (A) and lidar-derived building footprints that have been regularized using right angles (B), right angles and diagonals (C), and any angle (D). 35

Figure 20. Maps showing a comparison between 2015 orthoimagery (A) and lidar-derived building footprints that have been regularized using right angles (B), right angles and diagonals (C), and any angle (D). 36

Figure 21. A side-by-side comparison of the lidar-derived and provincial building footprints. 37

Figure 22. A comparison of a lidar-derived building footprint with 2015 provincial orthoimagery. Note the tree in the top right corner that partially covers the roof. 38

Figure 23. A cross-section of a building that is partly covered by high vegetation points. The location of the cross-section (B) is symbolized by a yellow line (A). 39

Figure 24. A cross-section of several buildings with adjacent or near-adjacent roofs. The location of the cross-section (B) is symbolized by a yellow line (A). 40

Figure 25. A building footprint that represents several buildings in very close proximity to one another. 40

Figure 31: Overview of the full Gaspereau River – Black River watershed INT raster to demonstrate issues with the data. Classified training area overlaid for context. 42

List of Tables

Table 1. GIS layers required for improved flood risk management efforts. 2

Table 2. List of LAS tile names acquired from GeoNova for the purpose of building classification. 5

Table 3. List of GeoNova lidar point classification values and descriptions. 6

Table 4. Summary of building classification and vectorization processing times..... 16

Table 5. Summary of different building footprint regularization processing times. 16

Table 6. Confusion matrix for CHM-INT classifier accuracy assessment (as seen in Figure 11B). 23

Table 7. Confusion matrix for CHM-INT hardwood vs softwood classifier accuracy assessment (as seen in Figure 11D)..... 23

Table 8. Summary of sixteen instances of missing building footprints. 24

Table 9. Summary of building classification limitations revealed by a more developed test area. 30

1 Introduction

1.1 Project Background

Flooding occurs when a large quantity of water exceeds its normal limits and overflows onto typically dry ground. The main causes of flooding in Nova Scotia have historically been heavy rainfall, melting snow, ice jams, storm surge, or a combination of all these factors (Province of Nova Scotia, 2017). In Nova Scotia and around the world, flooding is a natural phenomenon, but it can be a cause for concern when communities are affected, causing substantial damage to property (Thapa, et al., 2019). The development of effective flood prevention and monitoring solutions is critical in the adaptation to climate change and sea level rise.

Part of Nova Scotia's flood management planning is the Statement of Provincial Interest on Flood Risk Areas, which currently applies to five floodplains which have been identified under the Canada-Nova Scotia Flood Damage Reduction Program (Government of Nova Scotia, 1998). In the 1980s, these rivers were identified as having the highest flood risk in the province due to the amount of development along them at the time (Province of Nova Scotia, 2020). The Statement of Provincial Interest also noted that there are other flood-prone areas of the province that have yet to be mapped (Government of Nova Scotia, 1998). Flood risk areas are further distinguished into floodways and floodway fringes (Government of Nova Scotia, 1998). Within the floodplain, floodways are the areas that are most vulnerable to flooding. Flooding also occurs in these areas at the greatest depth and velocity. Floodway fringes describe the outer boundary of the flood-prone area, where there is less danger of flooding. These areas experience shallower and slower-moving floodwaters (Government of Nova Scotia, 1998; Province of Nova Scotia, 2020).

The province is seeking a better understanding of the impacts of dealing with existing structures in flood-risk areas and therefore want to develop more GIS analyses to enrich their flood risk analyses. Table 1 contains a list of GIS layers or rasters that will contribute to the province's flood management efforts; these are discussed further below.

Table 1. GIS layers required for improved flood risk management efforts.

GIS Layer	Information Contributed
Impervious surface layer	Data about objects and surfaces that change the course of water flow as the water cannot penetrate them.
Surface roughness grid	Provides apparent roughness metrics to support resistance calculations
Building footprints	Contribute structure information to impervious surface layer and roughness grids. Can also be used for damage projections.
Velocity grids	Show speed of water movement through the modelled flooded area.
Flood severity layer	Combine depth and velocity rasters to allow examination of flood extremes.

A provincial-scale impervious surface layer is required to more accurately quantify the amount of surface runoff and river discharge that occurs within different regions. Areas that have a high amount of impervious surface, such as in urban areas, are associated with a reduced hydrologic response time, leading to an overall increase in flooding risk (Feng, Zhang, & Bourke, 2021). A roughness grid is a crucial layer for assessing the impacts of existing structure in flood-prone areas. The layer represents the impedance to flowing water caused by objects and can be used to develop resistance parameters, such as Manning's n or M , that are used to adjust flow velocities. Impervious and smooth surfaces exhibit low resistance values compared to vegetated areas. This layer can be used to optimise the calibration and accuracy of hydrodynamic flood models (McGuigan, Webster, & Collins, 2015). Surface roughness grids can be generated through various methods including landcover classification and lidar-based feature height data (McGuigan, Webster, & Collins, 2015; Schubert, Sanders, Smith, & Wright, 2008). A better representation of water flow can be achieved by using building footprints in conjunction with roughness layers. For example, water flow is limited by small spatial dimensions around buildings in high density urban environments (Schubert, Sanders, Smith, & Wright, 2008). An accuracy assessment of lidar collected over floodplains can result in more robust roughness maps (Webster, Crowell, & Kodavati, 2020). Flood severity rasters combine the effects of depth and velocity by multiplying a depth raster by a velocity raster based on a specific flood event (FEMA, 2020). This critical layer for flood risk management requires data about water depth and velocity, which can be used to develop a threshold for flood severity distribution throughout a floodplain. Studies have used flood severity rasters to categorize floodplain areas into several hazard classes, ranging from low to extreme (Department of Municipal Affairs and Housing, 2022).

The Applied Geomatics Research Group (AGRG) was enlisted in the efforts to create GIS layers for flood management assessments and was tasked with developing a classification system specific to flood mapping that includes buildings. Existing data held by the Nova Scotia Government to update the classification of raw lidar data for a specific area to better position the province to be able to extend the work province-wide. The classification system was expanded to provide more detail on ground cover types in an effort to better represent significant features and improve hydrologic modelling accuracy. The results of this project will be used to make recommendations to improve the Statement of Provincial interest on Flood Risk Areas (Government of Nova Scotia, 1998).

1.2 Study Area Description

The study area was a 4 km² region within the Gaspereau River – Black River watershed (Figure 1). The Gaspereau River stretches approximately 24 km from its source at Gaspereau Lake to its mouth near Hortonville. There are several dammed sections in the upper reaches of the river that form deep, narrow channels. The lower reaches of the river are characterized by tidal marshes. A major tributary of the river is the Black River which connects to the Gaspereau River at White Rock (Millward, Ouellette, & Ricketts, 1985).

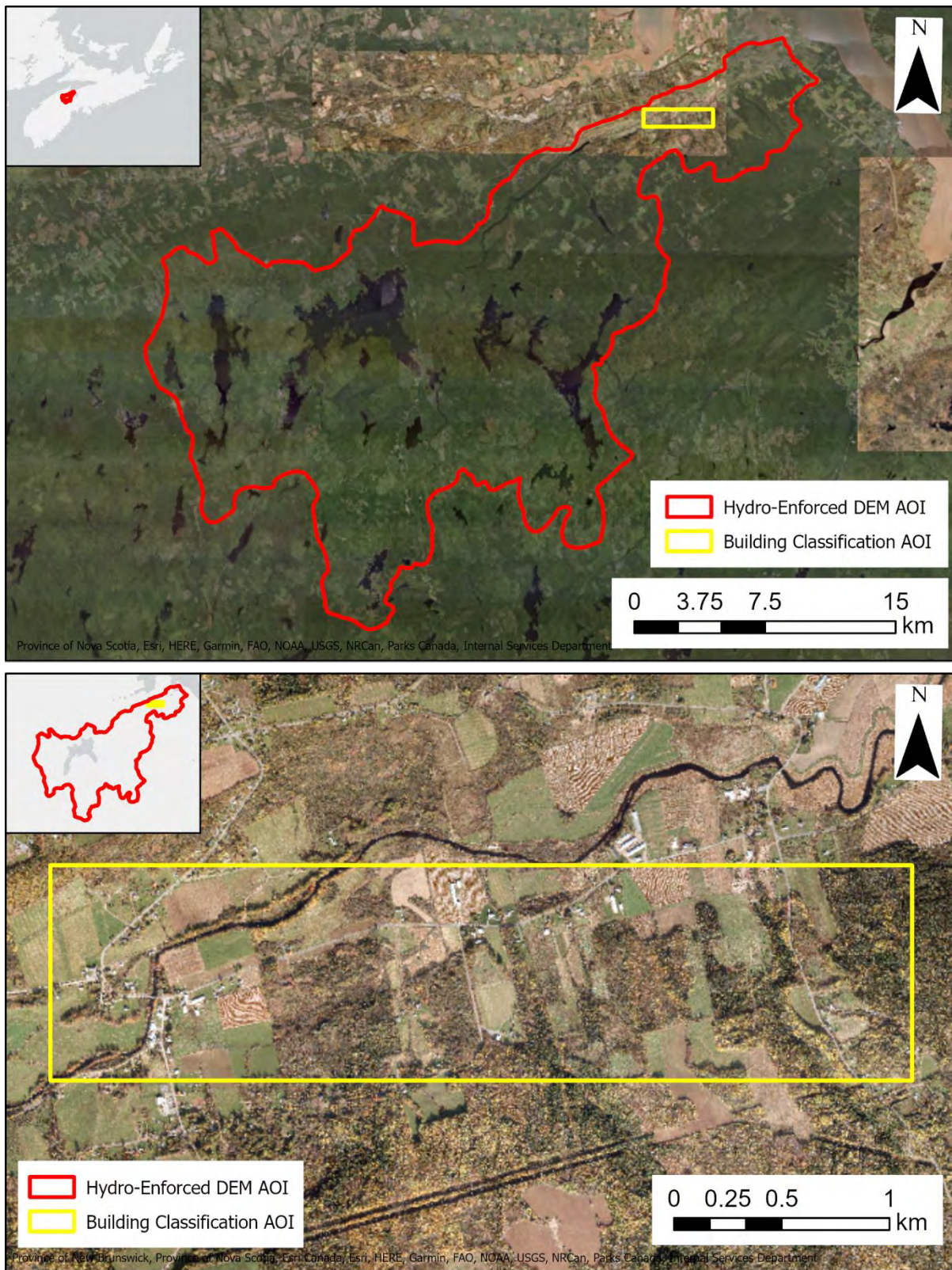


Figure 1. Maps of the study area used for the generation of hydro-enforced DEMs (top) and lidar classification updates for buildings and other land cover classes (bottom).

2 Methods

The following section describes the methodology used to update lidar classification for different land cover classes including buildings within the study area. Surface roughness layers were also produced. The processing time required for the building classification was recorded to estimate the level of effort required to expand the method province-wide.

2.1 Building Classification

2.1.1 Lidar Point Classification

Four neighbouring LAZ tiles (1 km²) within the Gaspereau watershed were obtained from GeoNova's Elevation Explorer. Lidar data was acquired with a long-range airborne laser scanner between July and August, 2020 (Table 2). The files were uncompressed to LAS files for compatibility with lidar processing software. Provincial building footprints were used to identify areas with a sufficient number of buildings to test the effectiveness of the automated classification routine. Additional criteria for the selection of lidar tiles included being situated in a floodplain and containing a variety of land cover classes.

Table 2. List of LAS tile names acquired from GeoNova for the purpose of building classification.

Product Name	Year	LAS Version	Horizontal Datum	Vertical Datum
393_4991_202001	2020	1.4	NAD83 CSRS (2010)	CGVD2013
394_4991_202001				
395_4991_202001				
396_4991_202001				

The Gaspereau River – Black River watershed contains primarily rural communities so further quality assessment of the automated building classification was conducted on several LAS tiles in the nearby town of Wolfville. This provided an opportunity to evaluate how well the classification performed on larger, more complex building roofs and more densely clustered housing.

GeoNova organizes their lidar points into discrete classes based on their physical characteristics, which have been summarized in Table 3. Building and structure points are grouped with trees in the high vegetation class (5).

Table 3. List of GeoNova lidar point classification values and descriptions.

Classification Value	Meaning
2	Ground
3	Low vegetation
4	Medium vegetation
5	High vegetation
9	Topographic water surface
17	Bridge deck

LAS files were imported into Terrascan, an application in the Terrasolid software family for managing and processing point clouds. All lidar classification steps were arranged in a macro for ease of processing. A full list of the steps used for classifying buildings within the selected LAS files are in the Appendix.

The lidar processing began by first temporarily removing points from the high vegetation class within 2 m above the ground class. This step was carried out so that points below the typical height of a building roof would not influence the identification of points by Terrascan. A building classification routine was then used to classify building roofs through the identification of planar surfaces above empty areas of the ground class. Echo information was included in the consideration of the building classification as points on roofs primarily belong to the echo type “only echo”. The minimum size of a building was defined as 40 m² and very strict classification rules were defined to prevent the classification of points belonging to nearby trees.

Beyond the initial building classification routine, several other classification steps were used to refine the identification of building points. As the building classification step tended to under-classify building points, a *Closeby* points routine was required to fill any gaps that existed in the roofs. After the building classification step was run, high vegetation points that belonged to the echo type “only echo” were temporarily moved to a reserved class. Another *Closeby* points routine was then run to classify points from the “only echo” high vegetation class to the building class based over several 3D search radiuses.

2.1.2 Building Footprints

The four LAS tiles with a newly added Building (6) class were exported from Terrascan and brought into ArcGIS Pro to extract a building layer that included elevation information. A LAS dataset with a projection of NAD 1983 CSRS UTM Zone 20N was defined to further process the classified data. The LAS dataset was filtered to only use the classified building points and was rasterized to generate a 0.5 m grid. During testing it was observed that using a cell size larger than 0.5 m resulted in many footprints being merged in cases

where buildings were in very close proximity to one another. The grid was then converted to an integer type before use in the Raster to Polygon tool. The resulting polygons were dissolved to leave only one polygon for every building.

Several tools were used to refine the building footprints. Some polygons were too small to correspond to real buildings, so they were removed from the building polygon layer based on having a shape area of less than 40 m². Small holes in the building footprints were filled by using the Eliminate Polygon Part tool; this was only done for areas less than 10 m². Jagged polygon borders, an artifact from converting the building lidar points to a raster, were smoothed using the Regularize Building Footprint tool. Different footprint regularization methods were explored, including methods for constructing polygons with 90° angles only, 45° and 90° angles, and using any angles identified between adjoining edges.

Elevation values referenced to CGVD2013 were assigned to each of the building footprints using zonal statistics. The Zonal Statistics as Table tool was used to calculate minimum, mean, maximum, and 95th percentile elevation values based on the newly generated building footprints and the building elevation raster. These values were joined to the building footprint layer by a common feature ID.

A spatial join was performed on the provincial building footprints and the lidar-derived building footprints to evaluate the quality of the automated classification routine. Buildings that were identified in the provincial footprint layer but not the lidar-derived layer were reassessed in Terrascan to help determine why they were omitted from classification. The lidar-derived footprints were visually compared to the provincial footprint layer and 2015 orthoimagery as an additional method of quality assessment.

2.2 Surface Roughness

The same four LAZ tiles used in the previous section were used to export 1 m resolution roughness layers from Terrascan. Terrascan defines surface roughness as the difference of a grid point from a plane fitted to the closest points in the source class. Therefore, the resulting grid represented the local elevation variation of points in the source class. The first roughness layer was produced using the Surface Roughness function on only the ground class. A second “roughness” layer was generated in Terrascan by calculating the vertical difference between the low vegetation class and the ground class. This step was repeated to export a layer containing height above ground information for medium vegetation. A greater vegetation height above ground value corresponded to a greater roughness value.

2.3 Land Cover Classification

A support vector machine (SVM) classifier was selected to segment and classify raster products derived from the lidar survey data. Common lidar products were used as model inputs including a digital elevation model (DEM), digital surface model (DSM), canopy height model (CHM), and an intensity raster (INT) raster (Figure 2).

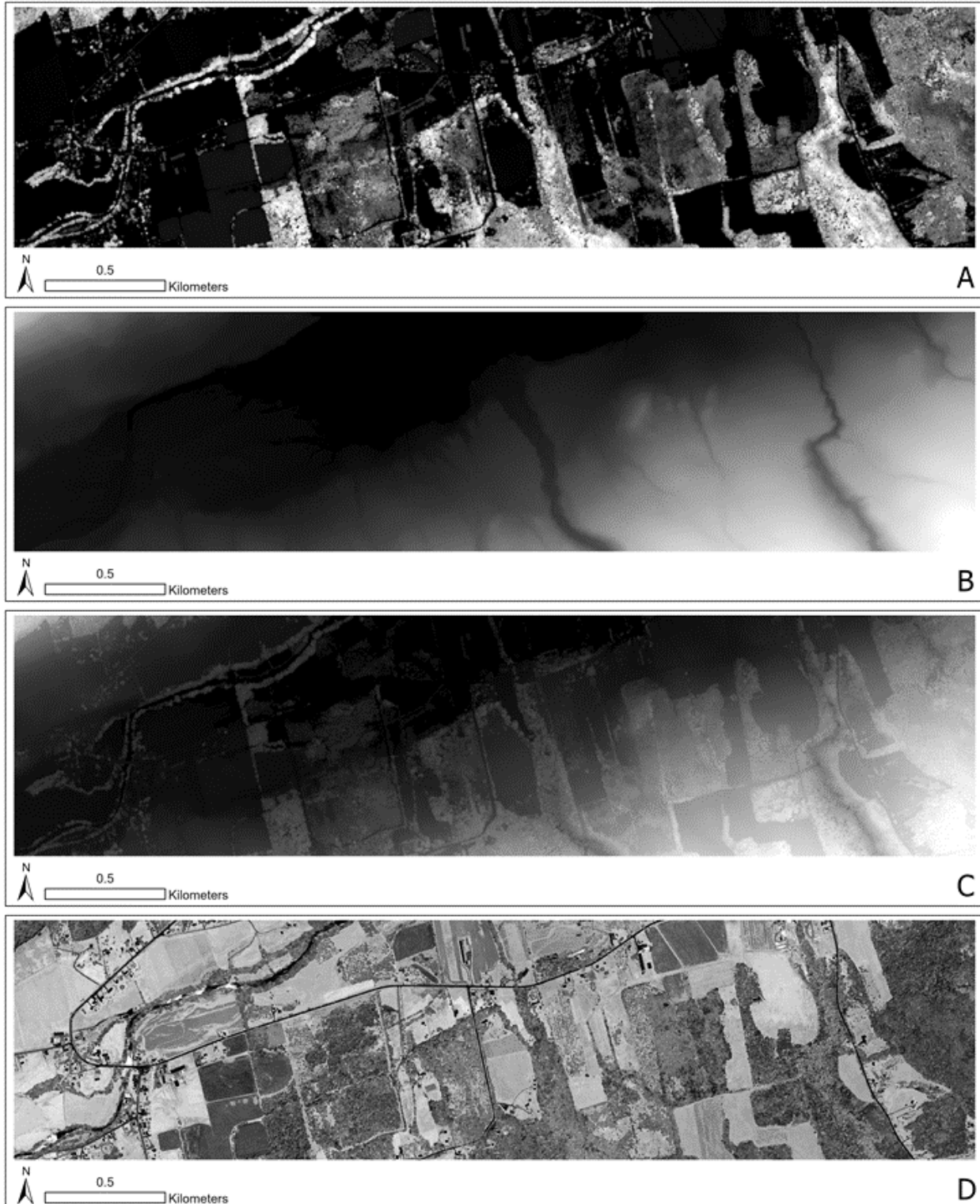


Figure 2. A comparison of potential lidar products to use as inputs to the SVM classifier. A: canopy height model (CHM); B: digital elevation model (DEM); C: digital surface model (DSM); and D: point return intensity (INT).

The SVM classifier within ArcGIS Pro only accepted three bands of raster input and it was essential to ensure each band provided unique data. It was important to maximize consistency between bands by ensuring that data were collected within a similar timeframe. Composite RGB orthophoto data were considered as a model input (Figure 3), however the temporal separation between the lidar and image data collections was problematic as areas were covered in vegetation in the lidar data but not the orthophotos. The imagery also contained several shadows throughout the scene that caused issues with the classification where shadows were wrongly classed due to their resemblance to other non-shadowed land cover types. These issues made the imagery unsuitable for use in classification and it was excluded from consideration.



Figure 3. An RGB composite orthophoto clipped to the classification training area.

A surface roughness estimate was also used as a model input and was generated using a raster function chain in ArcGIS Pro to extract curvature values from the DEM (Figure 4). The use of the roughness raster was investigated but consistently produced poor the results and was removed from consideration.

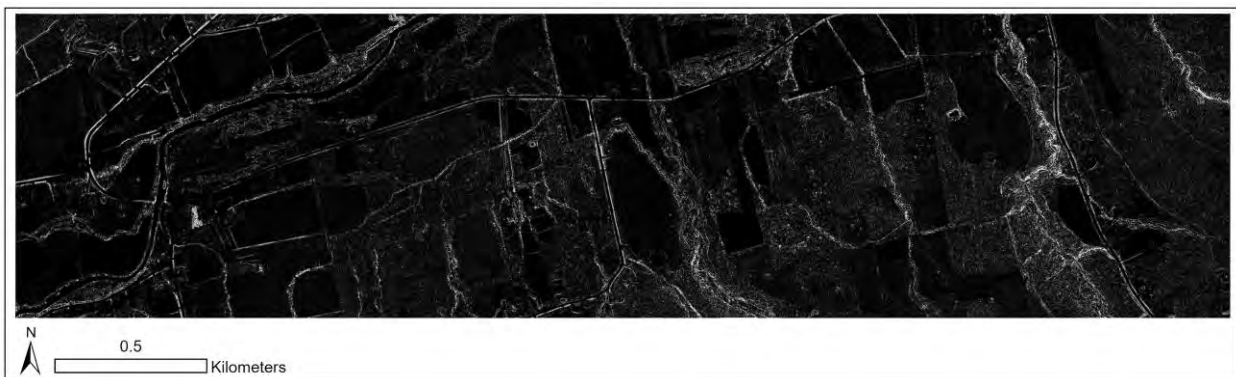


Figure 4. A roughness raster derived from the absolute value of the curvature of the DEM.

The SVM classifier is a supervised classification method and required classes to be defined and trained by selecting coverage areas within the data that were representative of each class. It was important to define an appropriate number of training sites for the defined classes. Excess training data resulted in an overfit SVM and reduced the external validity of the model outside the development site while too few training sites resulted in an underfit model that was unable to distinguish between similar landcover types.

3 Results

3.1 Building Classification

3.1.1 Lidar Point Classification

An automated building classification was performed using a Terrascan macro to classify building points in four LAS tiles obtained from GeoNova. The results of the building classification viewed in Terrascan are shown in Figure 5.

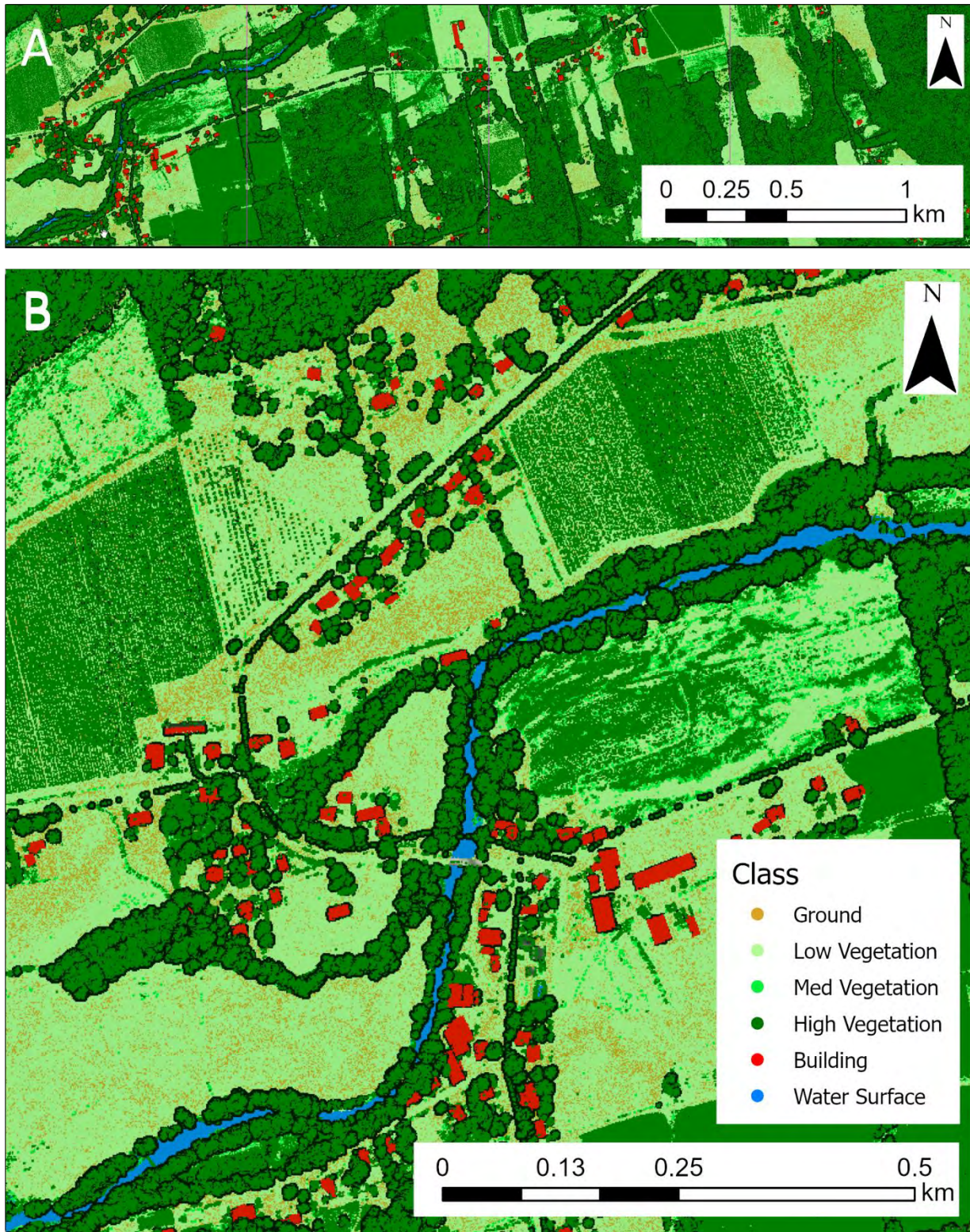


Figure 5. Result of automated building classification for the full extent of the study area (A) and in a single 1 km² tile (B).

3.1.2 Building Footprints

Classified building lidar points were used alongside ground returns to generate a 0.5 m DEM with buildings for the study area within the Gaspereau watershed. The resulting raster is displayed as a hillshade (Figure 6). Lidar-derived building footprints attributed with elevation information relative to CGVD2013 were produced from the elevation model. The automated building classification identified 173 buildings within the 4 km² study area (Figure 7).

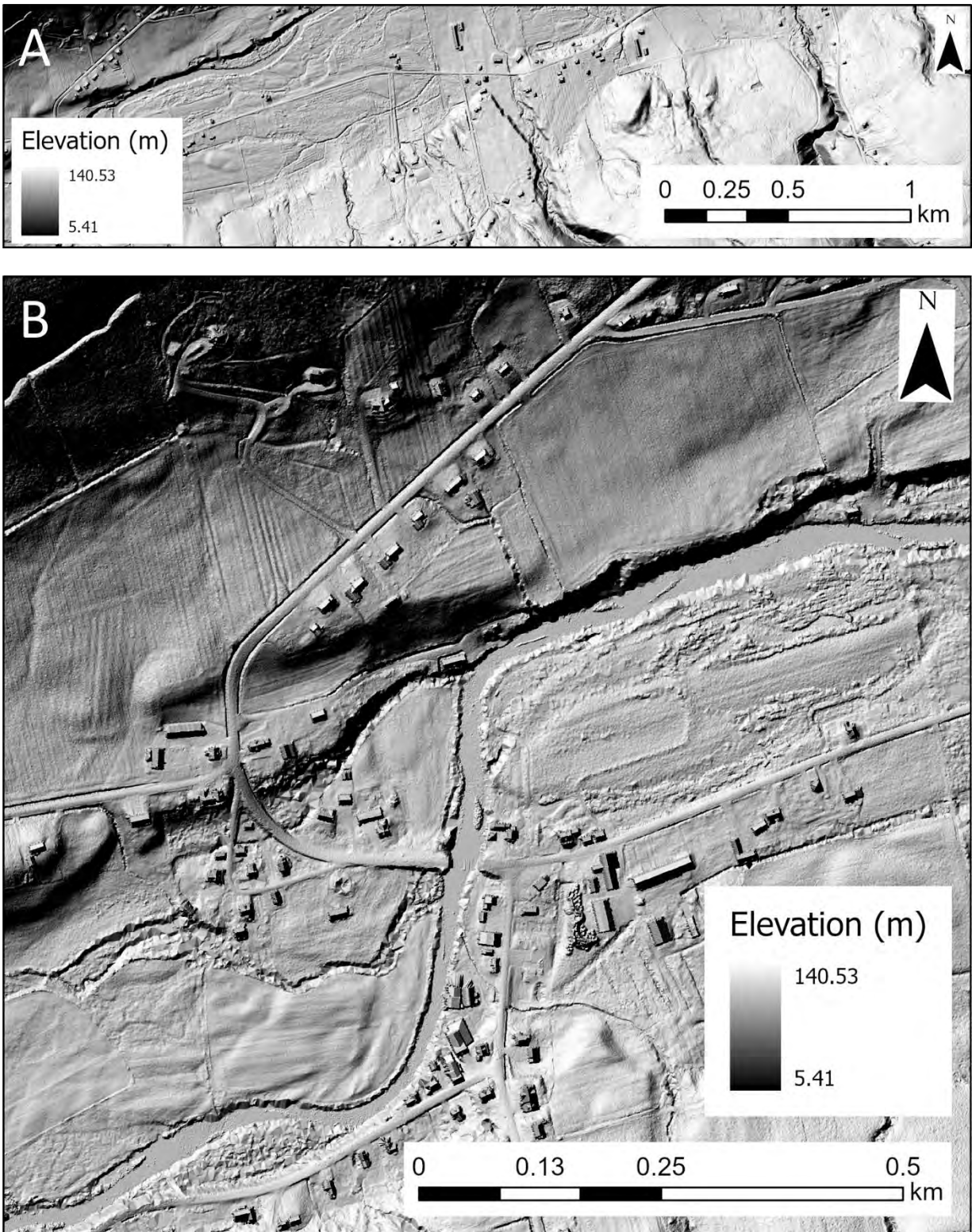


Figure 6. A digital elevation model of the study area containing ground and building lidar returns presented as a hillshade. The extent of the study area is displayed in (A) and a single 1 km² tile is displayed in (B).

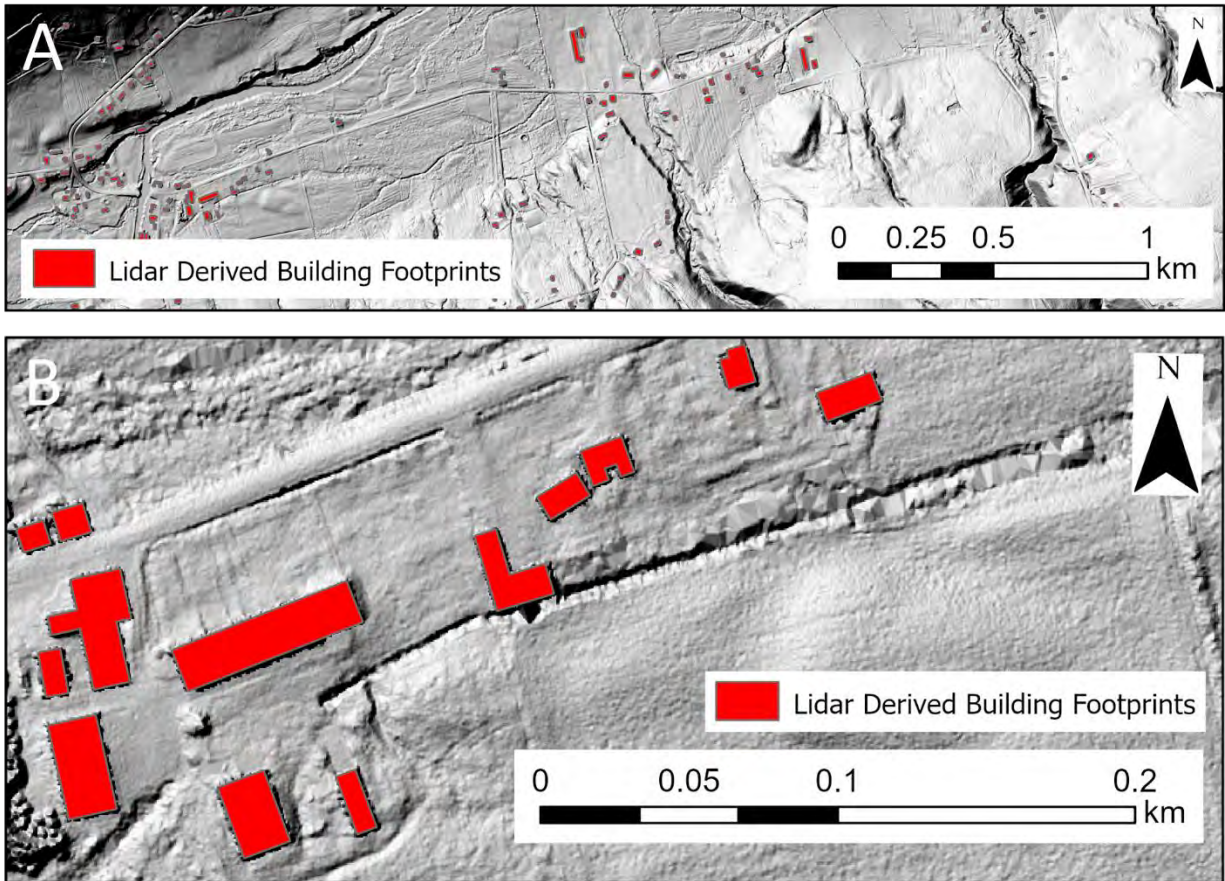


Figure 7. A map displaying building footprints that have been derived from an automated building classification routine. The extent of the study area is displayed in (A) and a closer view of the building footprints is displayed in (B).

3.1.3 Processing Time

Each processing step within the automated building classification routine and subsequent generation of building footprints was recorded to develop an estimation of the level of effort required to conduct the methodology on a provincial scale. For each processing stage, the time required to manually correct the automated results was also estimated. There are currently 66,366 1 km² LAS tiles that cover the province, however, there is some overlap between project years. The number of LAS tiles that cover the extent of the province without overlap was calculated by dissolving the lidar tile index for the province into a single polygon and calculating the resulting shape area. Using the assumption that each LAS tile is 1 km², the number of non-overlapping LAS tiles was calculated to be 62,746. The time it took to process the four LAS tiles within the study area alongside estimations of the amount of time required to complete to work province-wide is summarized in Table 4. The processing time for each of the three tested building footprint regularization methods is listed in Table 5.

Table 4. Summary of building classification and vectorization processing times.

Software	Processing Stage	Processing Time	
		Study Area (4 tiles)	Province-Wide (62,746 tiles)
Terrascan	Automated lidar point classification	6 minutes 13 seconds	~1,625 hours
	Manual lidar point classification	7 minutes	~1,830 hours
ArcGIS Pro	Automated building footprint generation (right angle/diagonal footprint regularization)	12 seconds	~52 hours
	Manual building footprint generation	10 minutes	~2,614 hours
Total		~35 minutes	~6,121 hours

Table 5. Summary of different building footprint regularization processing times.

Building Footprint Regularization Method	Processing Time	
	Study Area (4 tiles)	Province-Wide (62,746 tiles)
Right angles	11 seconds	~48 hours
Right angles and diagonals	12 seconds	~52 hours
Any angle	1 minute 4 seconds	~279 hours

3.2 Surface Roughness

Raw lidar data from GeoNova was used to produce layers that described the roughness of the bare earth (Figure 8), low vegetation (Figure 9), and medium vegetation (Figure 10) within the 4 km² study area. High surface roughness was observed around riverbanks, ditches along the side of the road, and portions of agricultural fields where heaps of soil are commonly stored. Higher roughness values corresponded to more resistance to flow. Low roughness values were observed on roads and bare earth agricultural fields. The lowest roughness values corresponded to smooth surfaces that have the least resistance to flow.

Surface flow is affected not only by the ground topography but also vegetation. Low vegetation (e.g., low-growing grasses and crops) and medium vegetation (e.g., tall grasses, shrubs) also represent less permeable surfaces than bare earth. Low and medium vegetation within the study area grew as high as 18 cm and 41 cm, respectively.

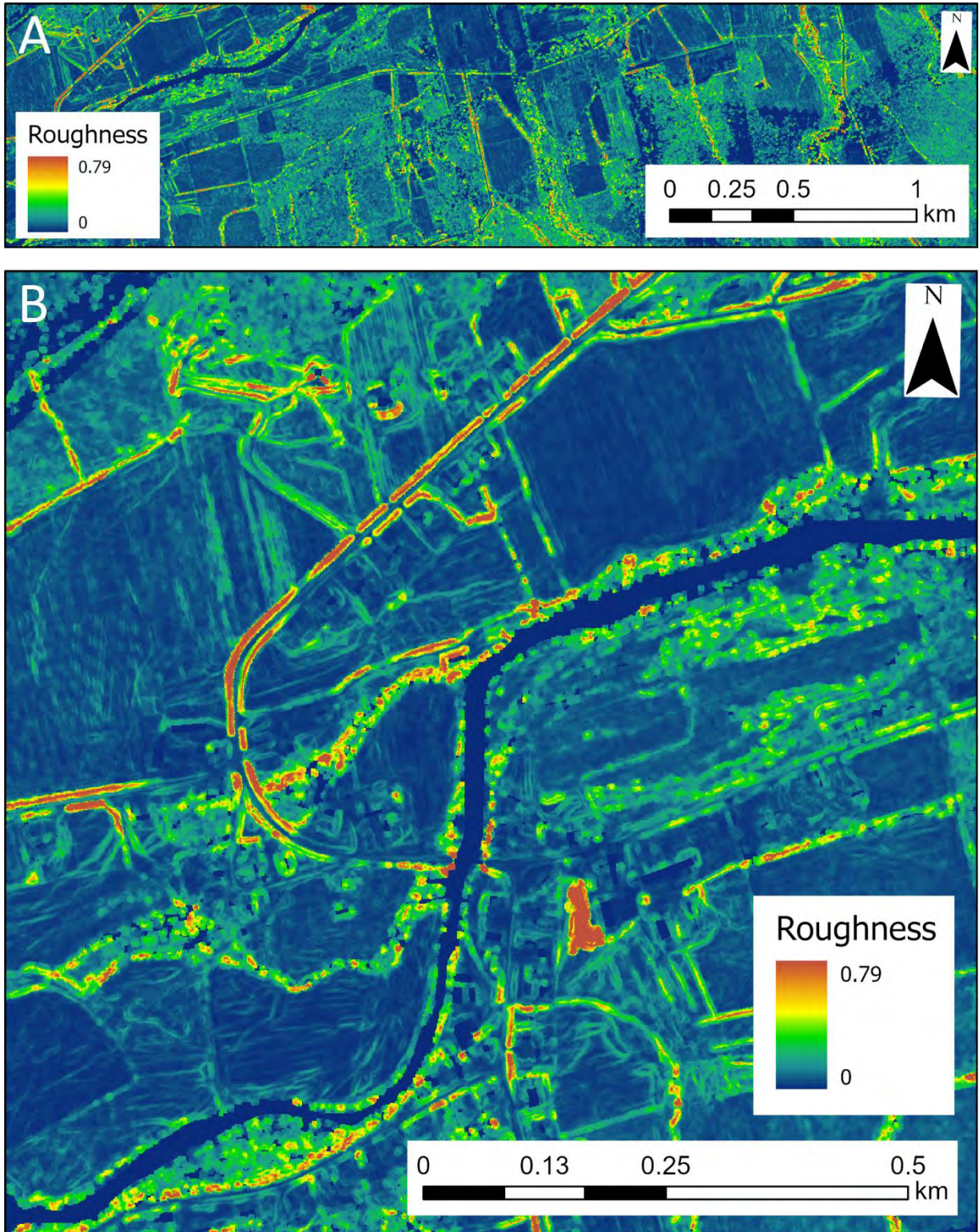


Figure 8. A surface roughness map generated from lidar ground returns for the full extent of the study area (A) and in a single 1 km² tile (B).

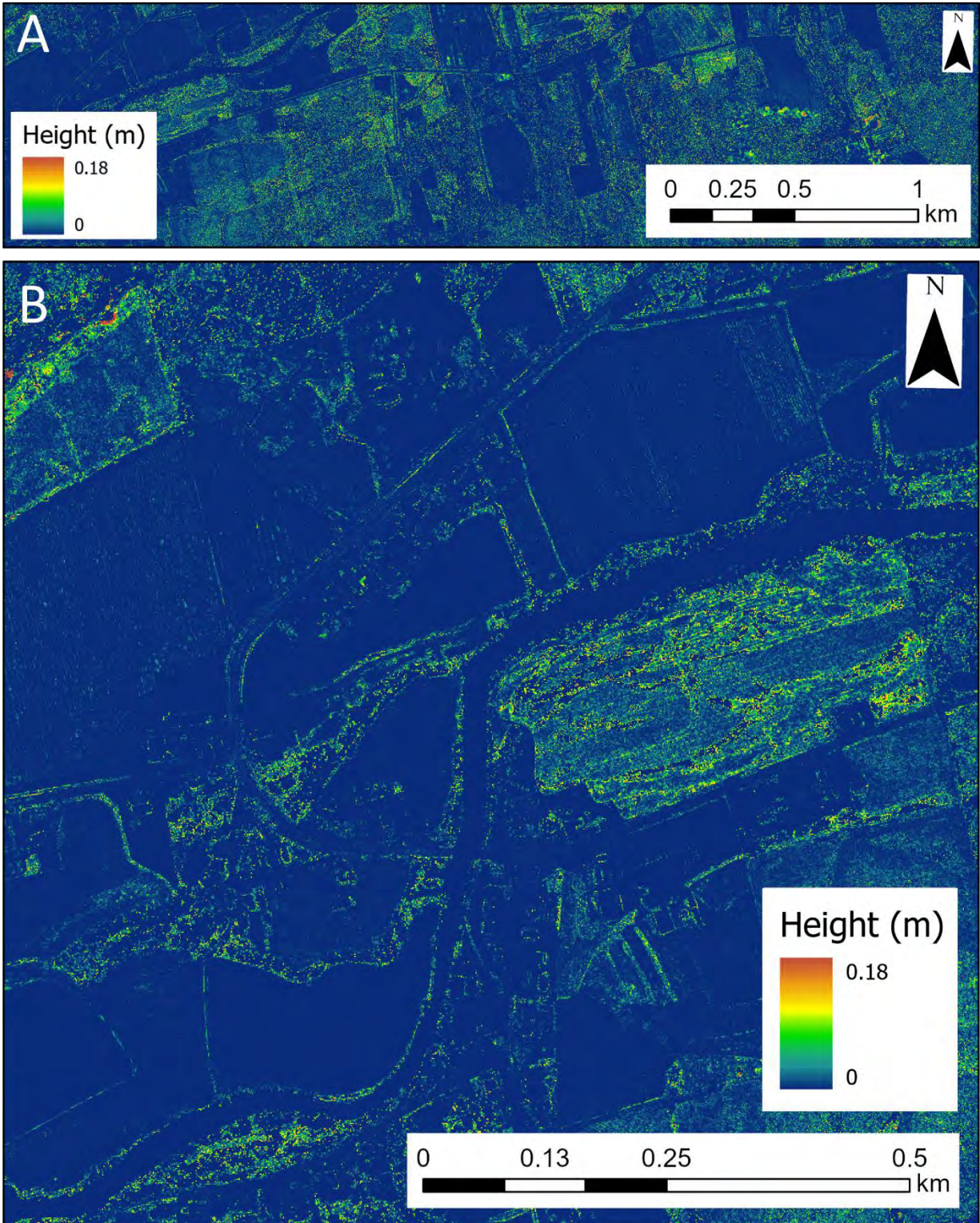


Figure 9. A map that represents the height of low vegetation above the ground class for the full extent of the study area (A) and in a single 1 km² tile (B).

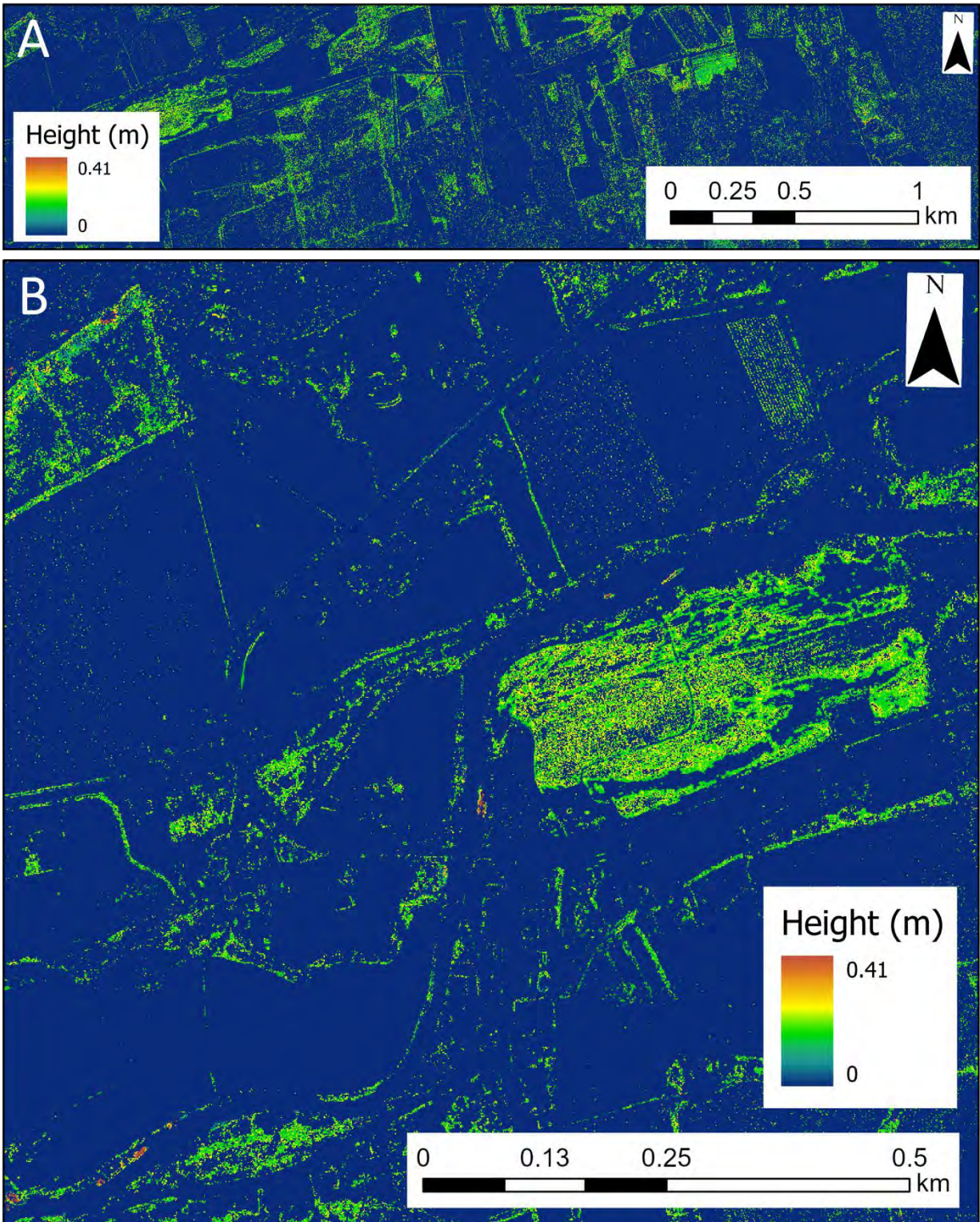


Figure 10. A map that represents the height of medium vegetation above the ground class for the full extent of the study area (A) and in a single 1 km² tile (B).

3.3 Land Cover Classification

3.3.1 Classifier Training

SVM results accuracies were assessed using random points within the validation data generated using the Create Accuracy Assessment tool within ArcGIS Pro. Confusion matrices were generated using the randomly sampled points to quantify errors between classes and identify problematic classes to guide model development in an iterative process. Initial results indicated that the CHM, DEM, and INT rasters produced acceptable SVM results (Figure 11). Further model iterations used only the CHM and INT rasters to determine the effect of the DEM's inclusion on the results as classes seemed to be unrelated to absolute elevation. The difference in results where the DEM was used (Figure 11A) or omitted (Figure 11B) were nearly imperceptible. When the roughness raster was added as an input the river was especially well classified, however each other class became inaccurate (Figure 11C). Based on the quality of the initial results additional forest training sites were added to the model and classes were defined for hardwood and softwood tree cover types. The added complexity did not negatively impact other classes and generated fewer misclassified building pixels in tree stands (Figure 11D).

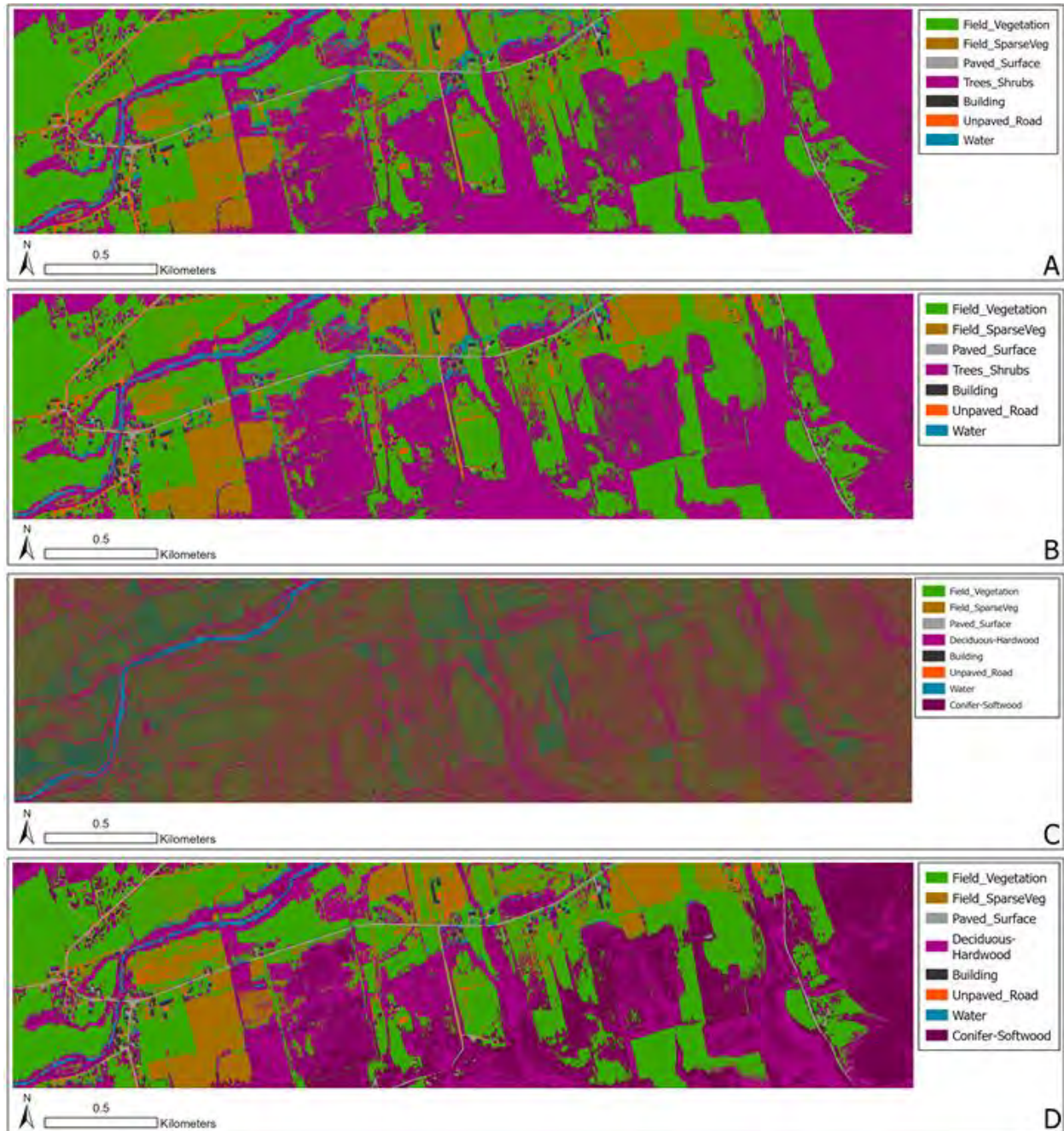


Figure 11. Results of four SVM classifiers, using different inputs and training data. A: CHM, DEM, and INT; B: Only CHM and INT; C: CHM, INT, and roughness; and D: CHM and INT with new training sites and distinction between soft and hardwood trees.

The iterative improvement process determined that the CHM and INT rasters provided the highest quality unique data to support classification. The CHM provided high contrast between the ground and tall objects such as buildings and trees, while the INT raster provided high contrast between areas of

vegetation, bare soils, and pavement. These were considered important factors when classifying impervious surfaces for the purpose of flood mapping (Figure 12).

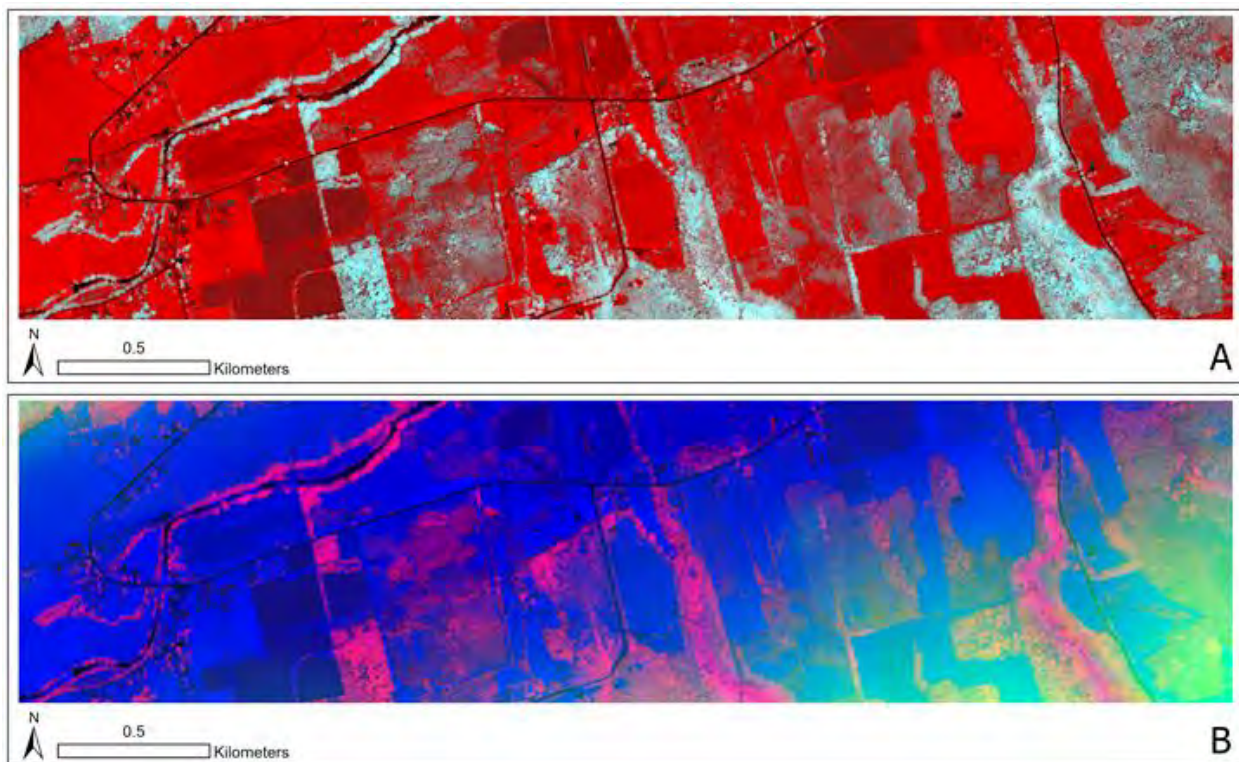


Figure 12. Two of the composites investigated for use with the SVM classifier. Note the colour change at the edges of B resulting from the inclusion of the DEM. A: Composite of the CHM and INT rasters; and B: Composite of the CHM, DEM, and INT rasters.

3.3.2 Accuracy Assessment

An accuracy assessment featuring a confusion matrix was performed on both the CHM-INT classification results with combined and distinct hard and softwood tree classifications. As the training site had no in-situ ground truth data or RGB imagery collected during the lidar flight a combination of the input lidar raster data, Google Earth satellite imagery, and a publicly available forest cover type shapefile from Nova Scotia's Department of Natural Resources were used for ground-truthing the ArcGIS Pro-generated accuracy assessment points.

The overall accuracy for the combined tree cover model was determined to be 59.3 percent (Table 6). Buildings and water were determined to be the weak points of this classifier. It was determined that inconsistent specular reflections in the river seen in the intensity layer caused confusion with other classes leading to water pixels being located throughout the image. False positives were problematic for the

building class. While real-world buildings were classified correctly, the assessed building classification accuracy was found to be 0 because several erroneous building pixels were included in the accuracy assessment. The overall accuracy for the separated tree class model was determined to be 65.9 percent (Table 7). Water was still a problematic class for the model, but building classifications were improved greatly. The improvement may have been a result of the greater number of training sites in forested areas that were required to distinguish between tree types.

Table 6. Confusion matrix for CHM-INT classifier accuracy assessment (as seen in Figure 11B).

		User-Interpreted Landcover							
		Field_Veg	Field_Sparse	Paved	Trees	Building	Unpaved_Rd	Water	Totals
Classified Landcover	Field_Veg	12	1	0	0	0	0	0	13
	Field_Sparse	0	10	0	0	2	0	1	13
	Paved	0	0	11	1	1	0	0	13
	Trees	0	0	0	13	0	0	0	13
	Building	0	0	1	12	0	0	0	13
	Unpaved_Rd	0	5	3	0	0	5	0	13
	Water	6	3	0	1	0	0	3	13
	Totals	18	19	15	27	3	5	4	N = 91

Table 7. Confusion matrix for CHM-INT hardwood vs softwood classifier accuracy assessment (as seen in Figure 11D).

		User-Interpreted Landcover								
		Field_Veg	Field_Sparse	Paved	Hardwood	Build	Unpaved_Rd	Water	Softwood	Totals
Classified Landcover	Field_Veg	11	0	0	0	0	0	0	0	11
	Field_Sparse	1	9	0	1	0	0	0	0	11
	Paved	1	0	8	0	1	1	0	0	11
	Hardwood	1	0	0	8	0	0	0	2	11
	Build	0	0	0	3	8	0	0	0	11
	Unpaved_Rd	1	3	0	0	0	7	0	0	11
	Water	6	0	0	1	0	1	3	0	11
	Softwood	1	2	0	4	0	0	0	4	11
	Totals	22	14	8	17	9	9	3	6	N = 88

4 Discussion

4.1 Building Classification

4.1.1 Lidar Point Classification

4.1.1.1 Study Area

The primary study area for the automated building classification was a rural community located in the Gaspereau watershed. A spatial join determined that 18 buildings of the 173 buildings identified by the automated routine were not present in the provincial database. 15 of these buildings were present in the 2015 provincial orthoimagery, however they were not digitized. The remaining three buildings were built after the provincial orthoimagery was collected, as confirmed by identifying their locations in 2021 satellite imagery.

The provincial building footprint layer had identified 172 buildings within the study area. Another spatial join was conducted to verify the accuracy of the automated classification process. It was revealed that 16 buildings out of the 172 identified in the provincial building footprint layer were not present in the lidar-derived footprints. It was possible to explain each instance of potential misclassification through reinspection of the point clouds in Terrascan. Table 8 presents a summary of the instances, which are then discussed in further detail.

Table 8. Summary of sixteen instances of missing building footprints.

No of Buildings Misclassified	Explanation
6	Building not present in point cloud
4	Insufficient point density for building classification
3	Occlusion (complete or partial) of building
3	Structure smaller than defined parameter

The biggest source of missing footprints discovered during verification of the classification procedure was simply that the buildings were not present in the point cloud. Six buildings fell into this category, as confirmed by taking cross-sections corresponding to the location of each missing building footprint. Of these six buildings, five were also absent in the 2015 orthoimagery used to digitize the footprints. It is unknown why one building was present in the orthoimagery but absent in the digitized provincial footprints. Figure 13 and Figure 14 display the location and cross-section of a building absent in the orthoimagery but identified by the province.

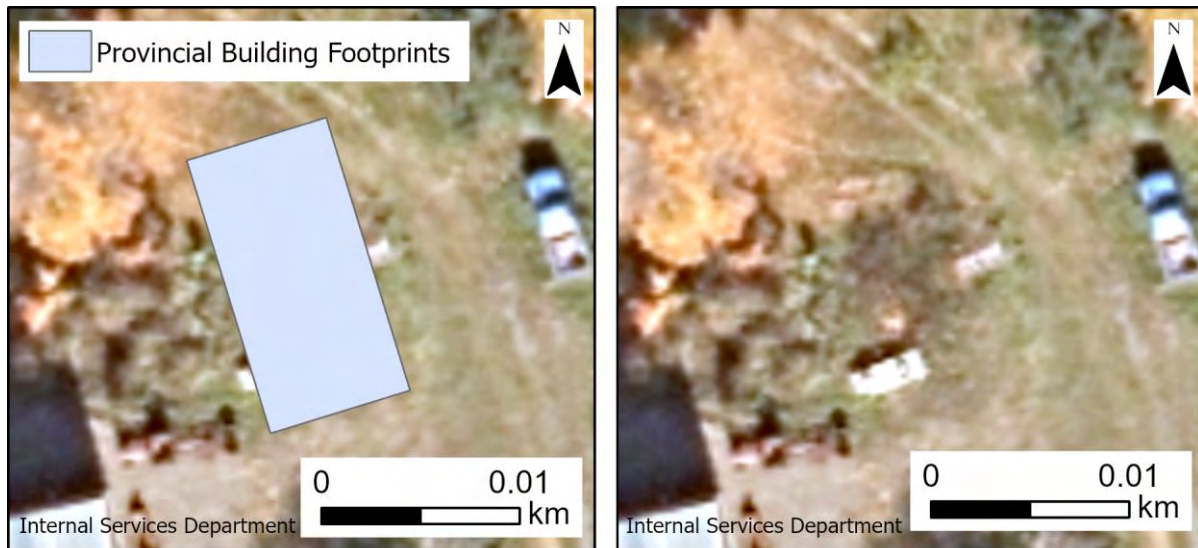


Figure 13. A comparison of a building footprint identified by the province with the 2015 orthoimagery used to digitize it.

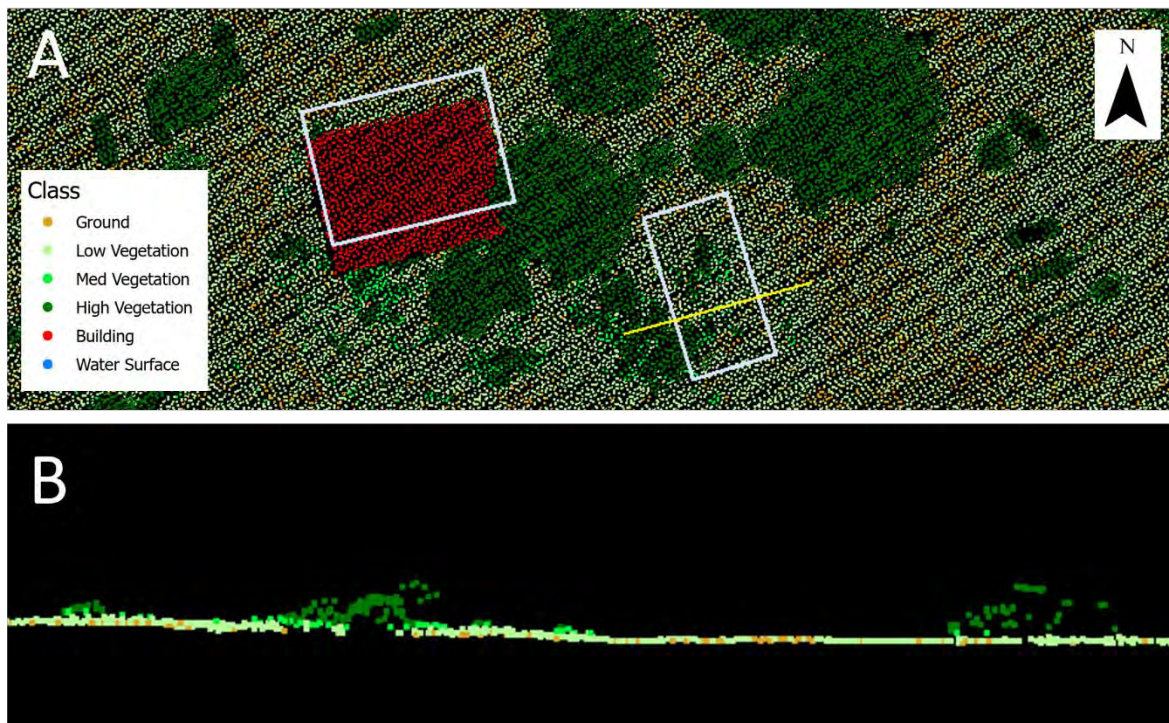


Figure 14. A cross-section of a building as identified by the province but not visible in the point cloud. The location of the cross-section (B) is symbolized by a yellow line (A). Provincial building footprints are symbolized with a white polygon (A).

Four buildings could not be classified with the automated routine due to a sparsity in high vegetation points corresponding to buildings. Figure 15 shows a cross-section of a building with insufficient point density for classification. Asphalt shingles do not generally produce high amplitude lidar returns as a large portion of the pulse energy is absorbed or reflected away from the sensor. Consistent collection of these features requires proper system operation and an adequate lidar pulse strength.

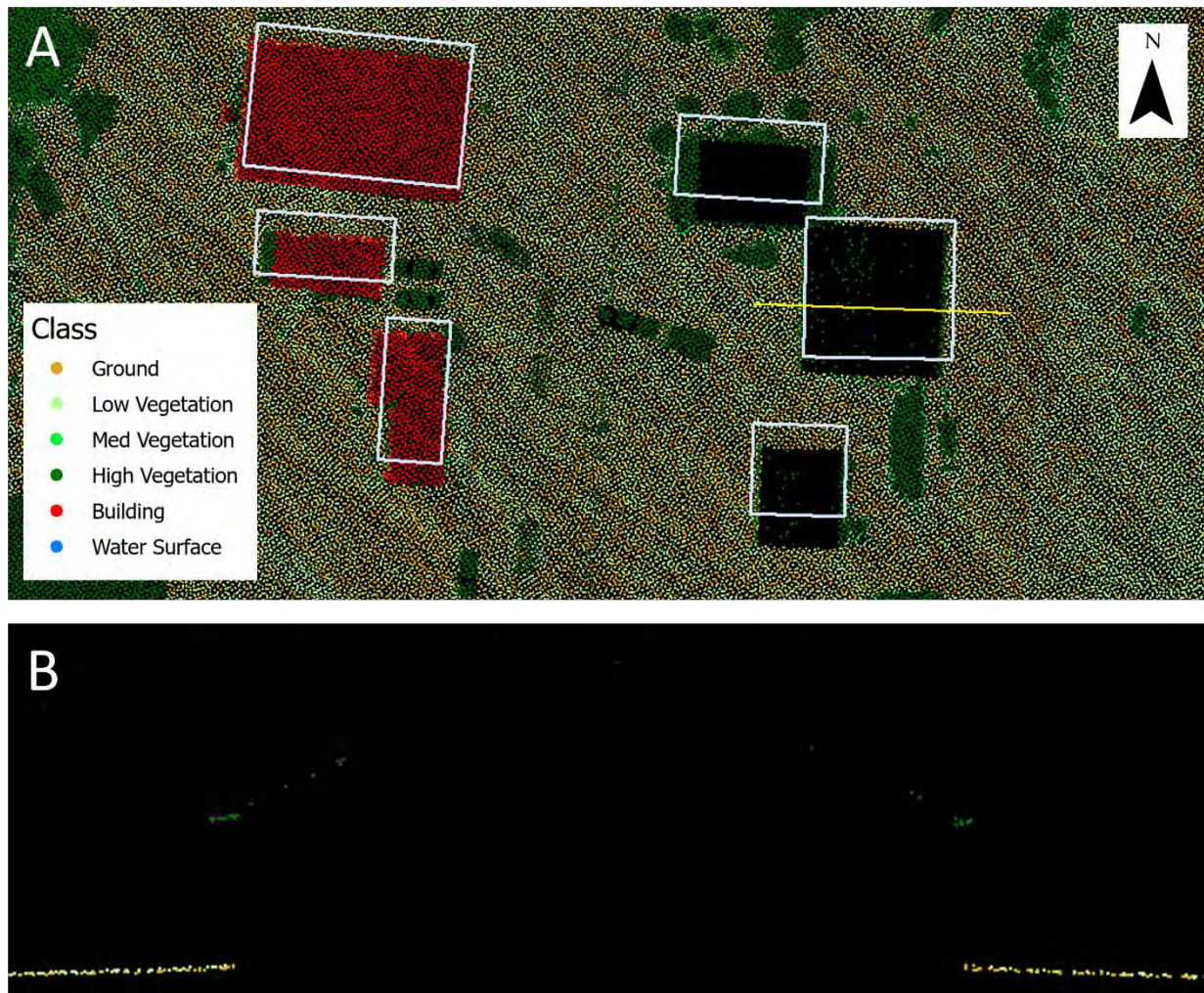


Figure 15. A cross-section of a building that was excluded from the automated building classification due to sparse lidar points. The location of the cross-section (B) is symbolized by a yellow line (A). Provincial building footprints are symbolized with a white polygon (A).

Three buildings were not classified by the automated classification routine due to partial or complete occlusion of building points. Figure 16 shows the location of a building that could not be identified by the classification routine due to partial occlusion of the roof by trees.

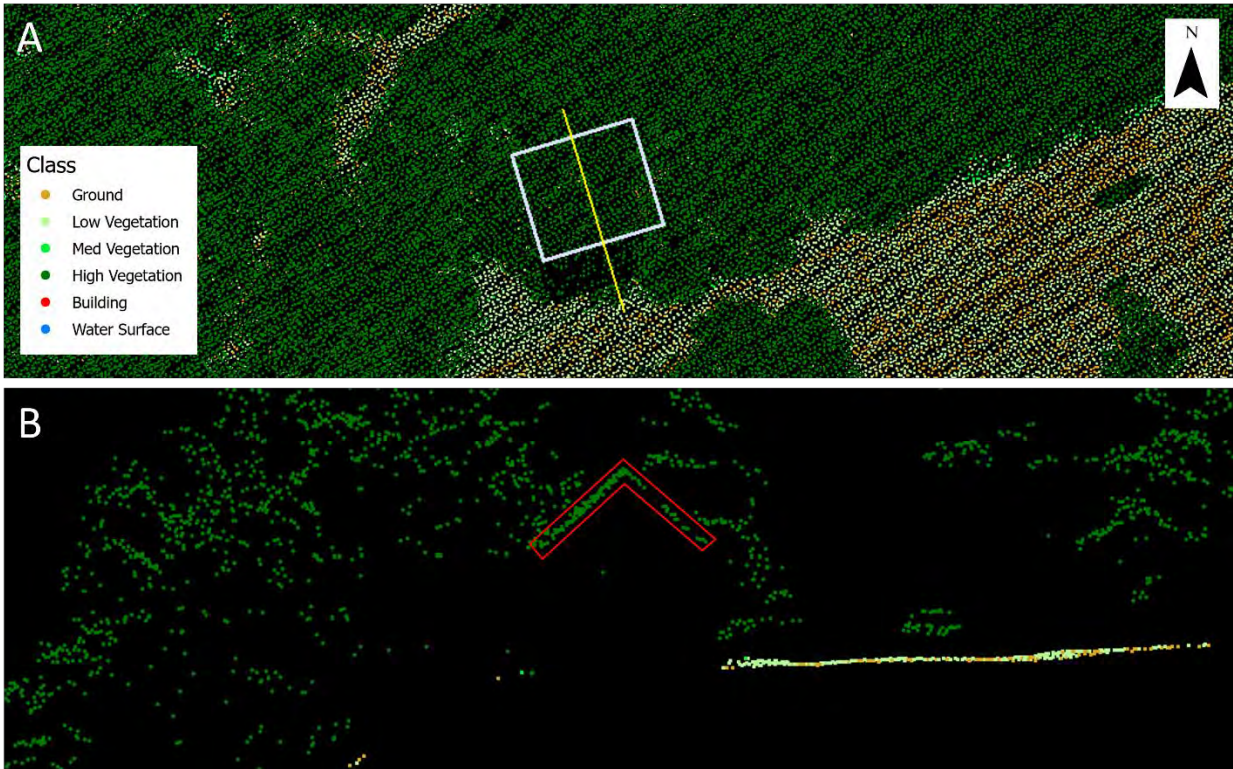


Figure 16. A cross-section of a building left unclassified by the automated routine due to partial occlusion of the roof. The location of the cross-section is symbolized by a yellow line (A) and the probable location of building points is outlined in red (B). Provincial building footprints are symbolized with a white polygon (A).

Finally, three buildings were not classified due to being too small (<40 m²) to be identified by the classification routine. Figure 17 shows the location of a building approximately 30 m² in size.

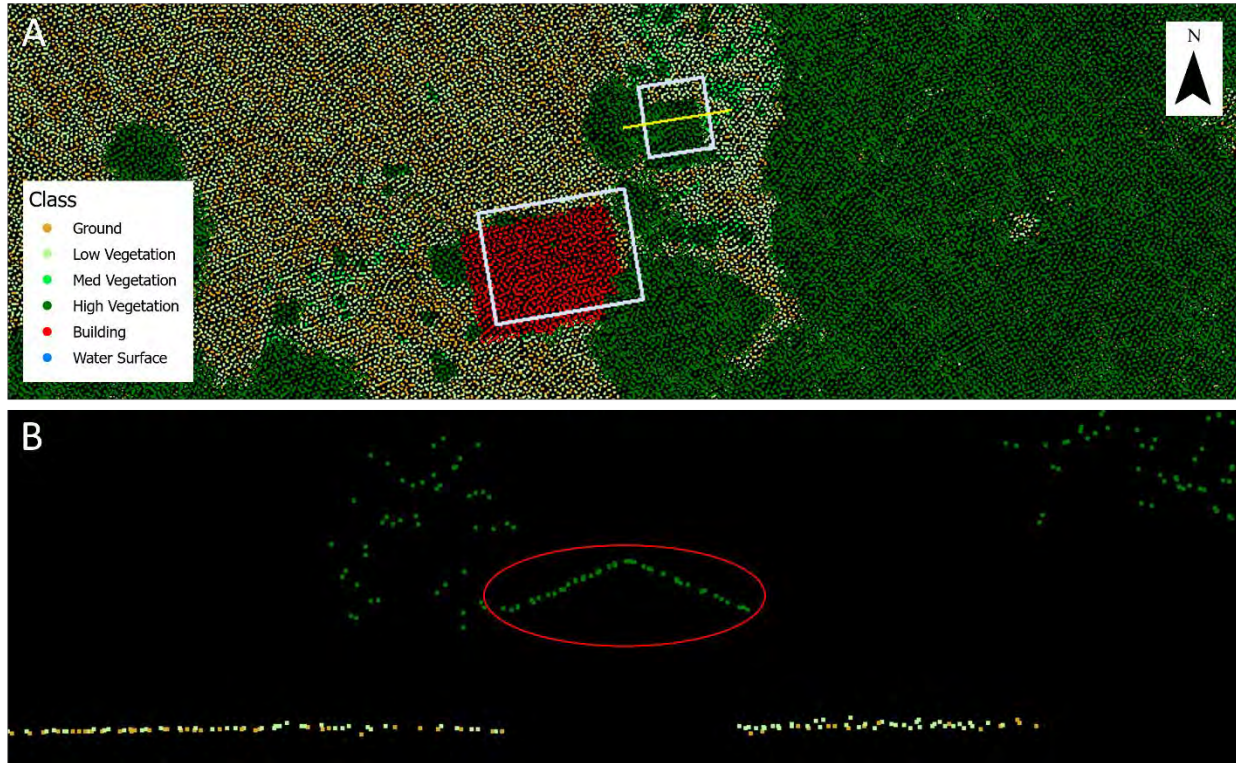


Figure 17. A cross-section of a building that was too small to be identified by the classification routine. The location of the cross-section is symbolized by a yellow line (A) and probable building points are circled in red (B). Provincial building footprints are symbolized with a white polygon (A).

The building classification routine was tested using parameters that ranged from very strict to very relaxed for how closely the points must follow a planar surface. It was determined that using strictest possible rules resulted in the fewest amount of erroneously classified points, therefore, decreasing the amount of time required for manual classification without significantly increasing the total processing time (Figure 18).

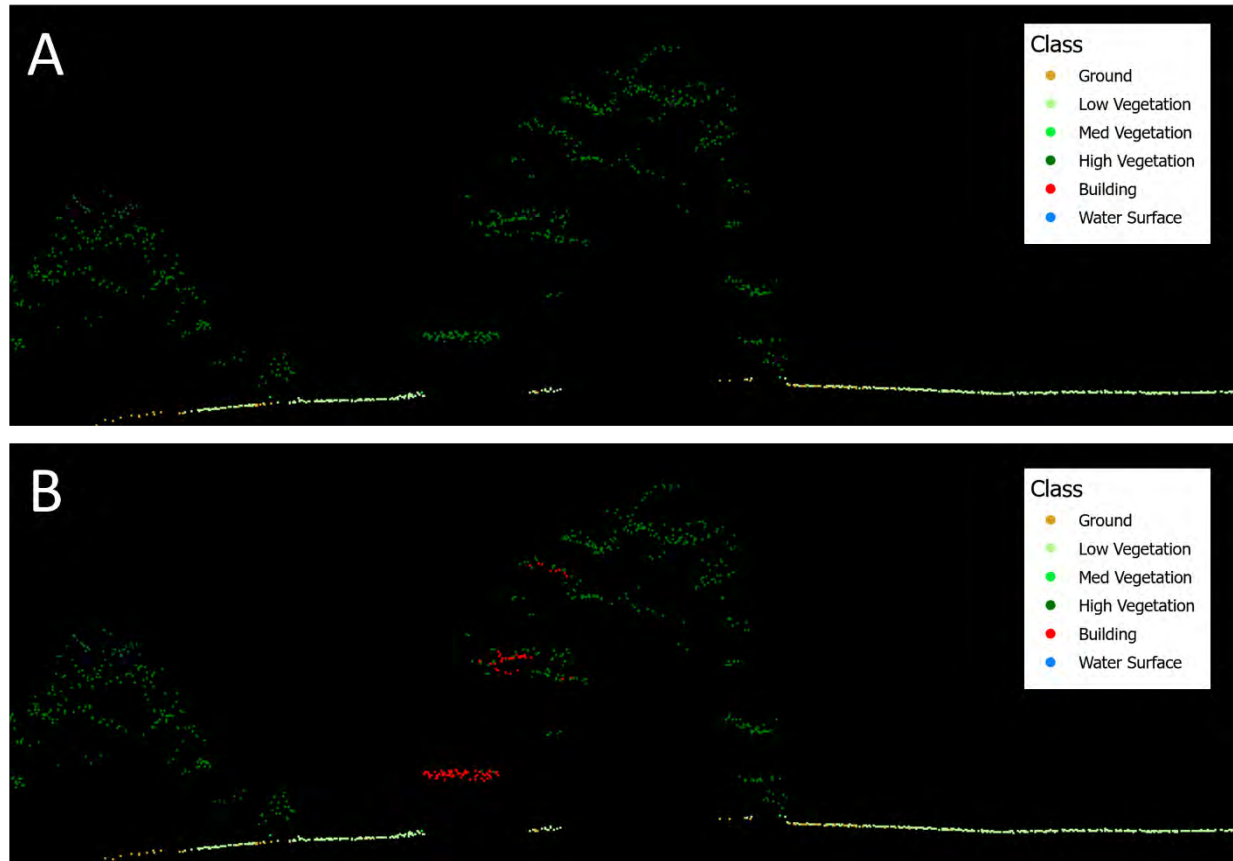


Figure 18. A cross-section of a tree after the automated building classification was conducted with a Very Strict parameter (A) and a Strict parameter (B).

4.1.1.2 Expanded Assessment Area

Further assessment of the classification accuracy was conducted in the nearby town of Wolfville which had a higher density of houses and commercial buildings. Overall, the automated classification routine provided similar results in terms of identifying building points, however, additional limitations of the classification were revealed, as summarized in Table 9. For example, the automated building classification routine had a reduced capacity to detect buildings with large changes in slope due to the strict nature of the acceptance parameters. Figure 19 shows the steeple of a church left unclassified by the automated routine.

Table 9. Summary of building classification limitations revealed by a more developed test area.

Issue	Result
Large changes in slope of building	Misclassification of structure (church steeple)
Noise from transparent materials	Greenhouses not properly classified
Erroneous ground points	Portion of roofs excluded from classification
Cluster of vegetation of uniform height within building parameters	Misidentified as building

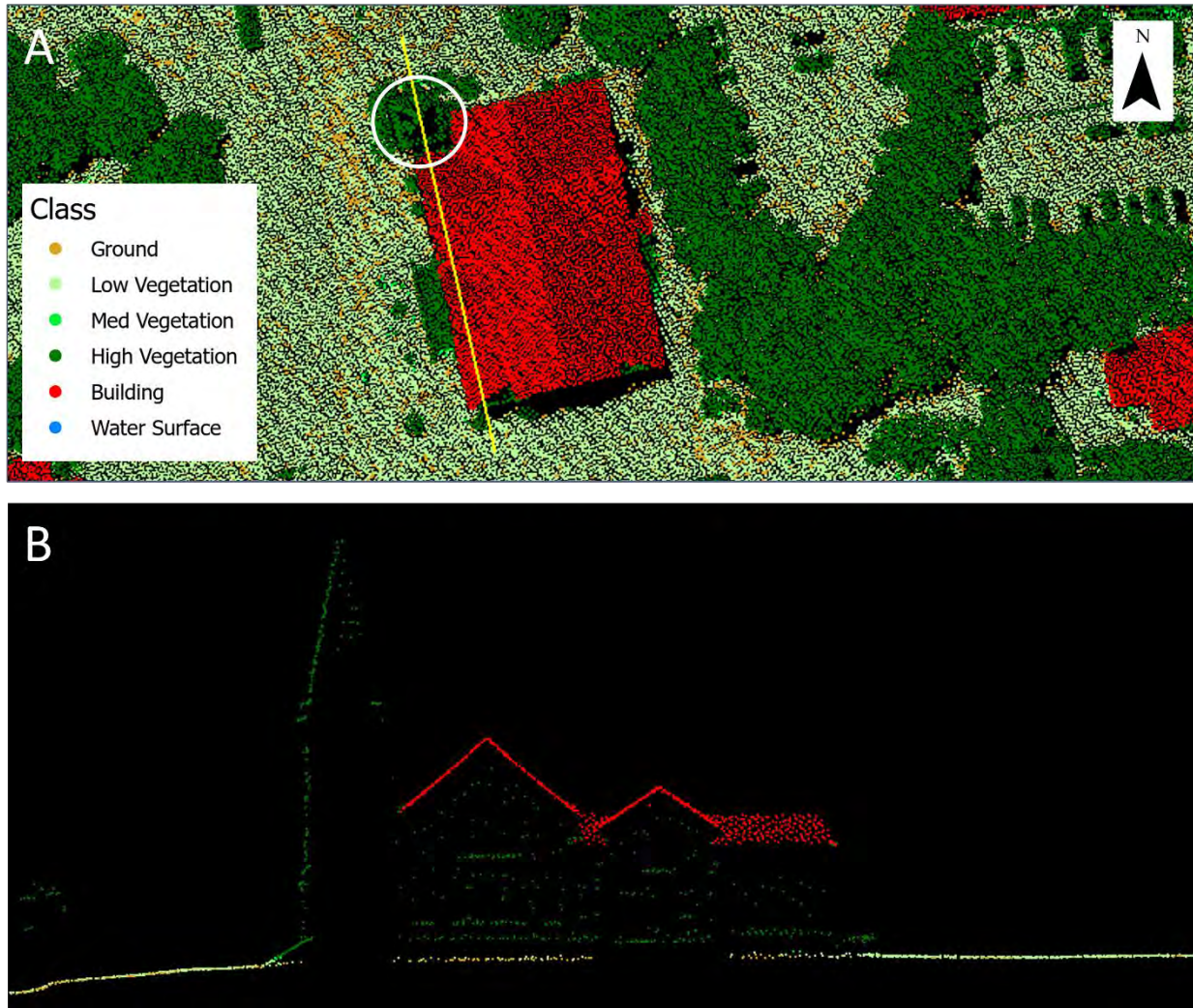


Figure 19. A cross-section of a church. The location of the cross-section (B) is symbolized by a yellow line (A). The location of the church steeple is circled in white (A).

Data collected by lidar sensors in an environment with transparent or specular reflective surfaces are subject to significant noise produced by the reflection of objects near the transparent material. As such,

greenhouses failed to be accurately classified by the automated routine due to an inability to detect a planar surface (Figure 20).

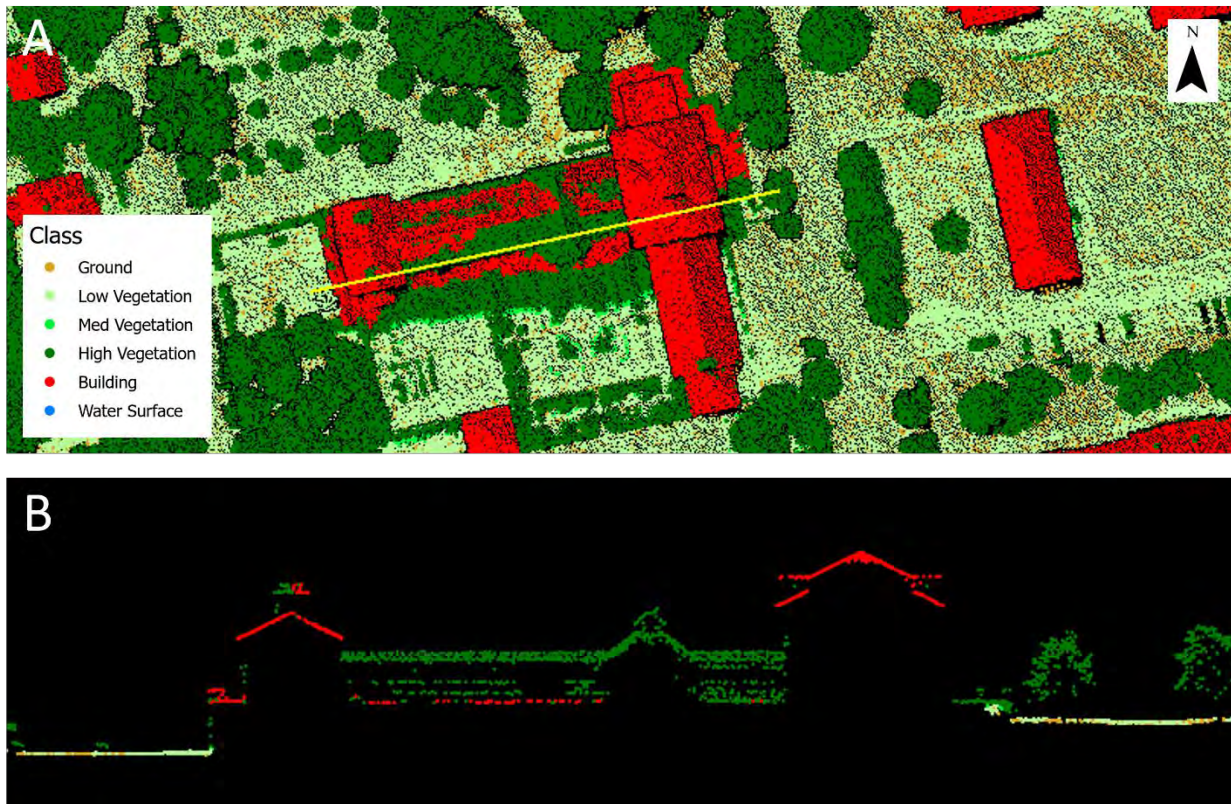


Figure 20. A cross-section of a greenhouse that failed to be accurately classified by the automated routine. The location of the cross-section (B) is symbolized by a yellow line (A).

As the detection of building points was based on empty areas in the ground class, an instance was noted where the presence of ground points led to a portion of a roof being excluded from classification (Figure 21). The accuracy of the ground classification was determined to be a critical variable for the building classification routine with difficulties arising when single LAS tiles contained data collected over a relatively large timeframe.

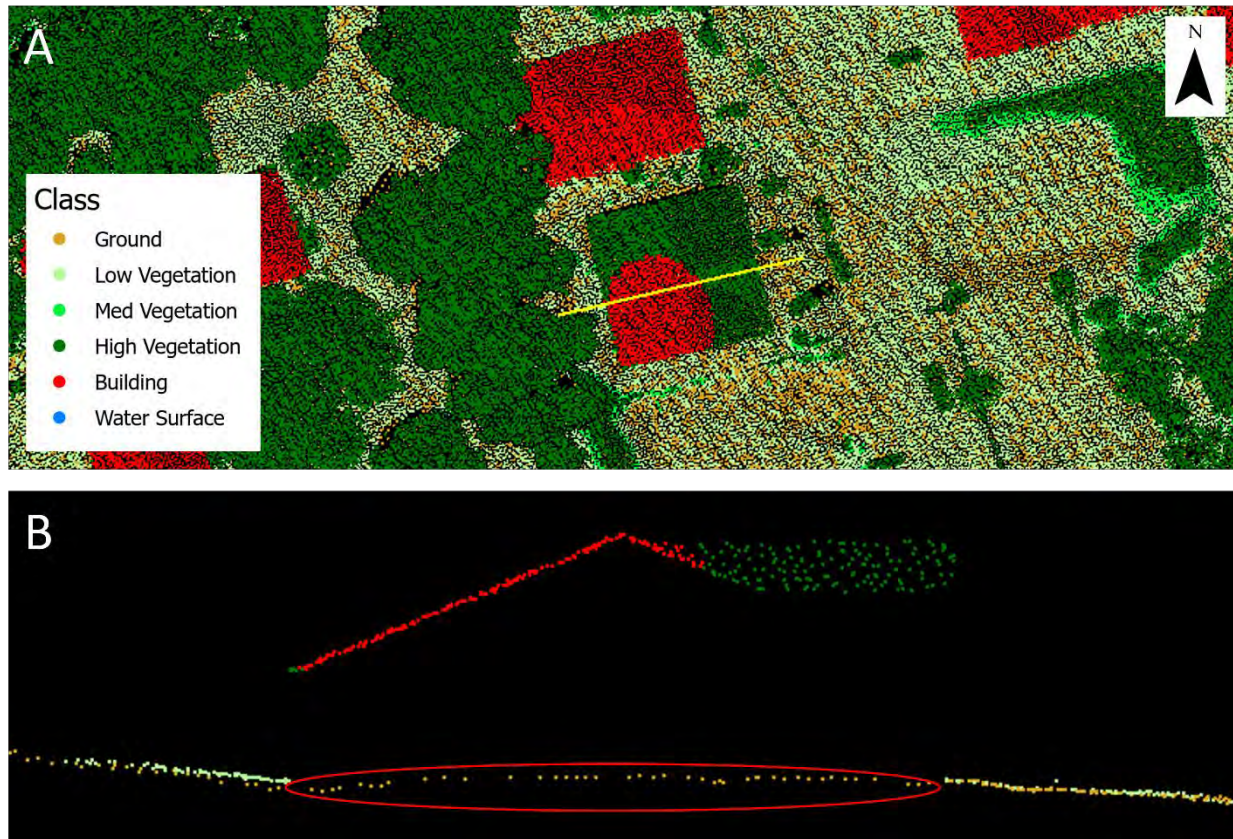


Figure 21. A cross-section of a building that was not entirely identified by the automated classification routine due to erroneous ground points underneath the building points. The location of the cross-section is symbolized by a yellow line (A) and ground points are circled in red (B).

An instance of misclassification was observed where a dense cluster of high-vegetation points was classified as a building. A likely explanation for this error in classification is that the vegetation had a fairly uniform height, resulting in the routine detecting a planar surface (Figure 22; Figure 23).

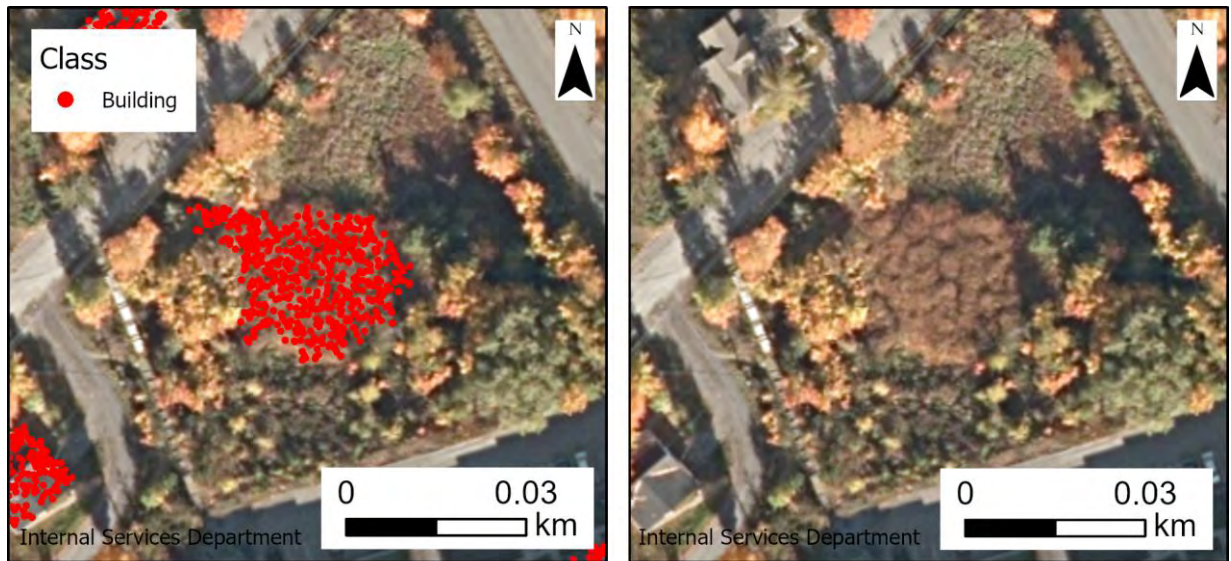


Figure 22. Maps showing the location of a group of misclassified building points in comparison to 2015 orthoimagery.

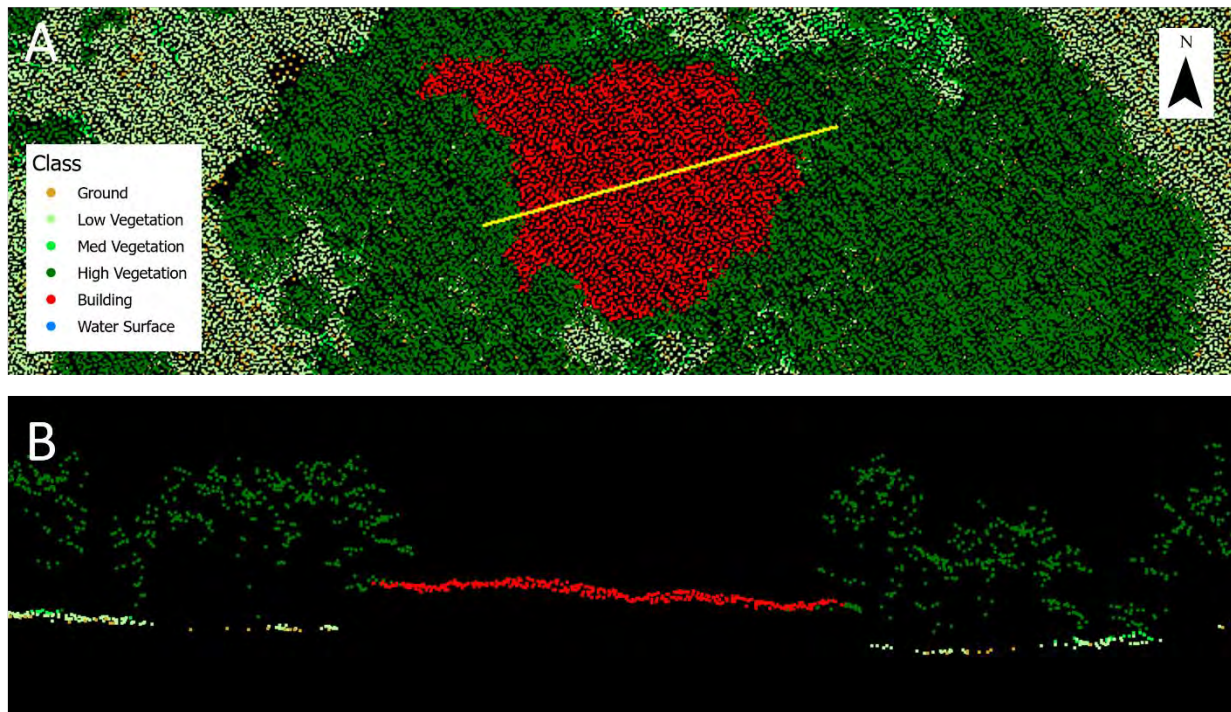


Figure 23. A cross-section of dense vegetation misclassified as a building by the automated routine. The location of the cross-section (B) is symbolized by a yellow line (A).

4.1.2 Building Footprints

4.1.2.1 Study Area

Elevation values were attributed to the building footprints using the minimum, mean, maximum, and 95th percentile elevation of the classified building points. It was determined that using the 95th percentile values would be most representative of the building's true elevation as any erroneously classified points (e.g., belonging to a nearby tree) would have less influence over the calculated elevation.

Different building footprint regularization methods were explored with the Regularize Building Footprint tool. The right angles method had the quickest processing time (Table 5), however, it was found to have a tendency to overgeneralize building footprints. Incorporating both 45° and 90° angles in the generation of polygons resulted in footprints that matched irregular building roofs more accurately. Allowing the construction of polygons using any identified angles, on the other hand, resulted in irregular footprints that didn't necessarily match the actual shape of the building roof. This method also required the most processing time and computational resources. Figure 24 and Figure 25 display a comparison of different building regularization parameters.

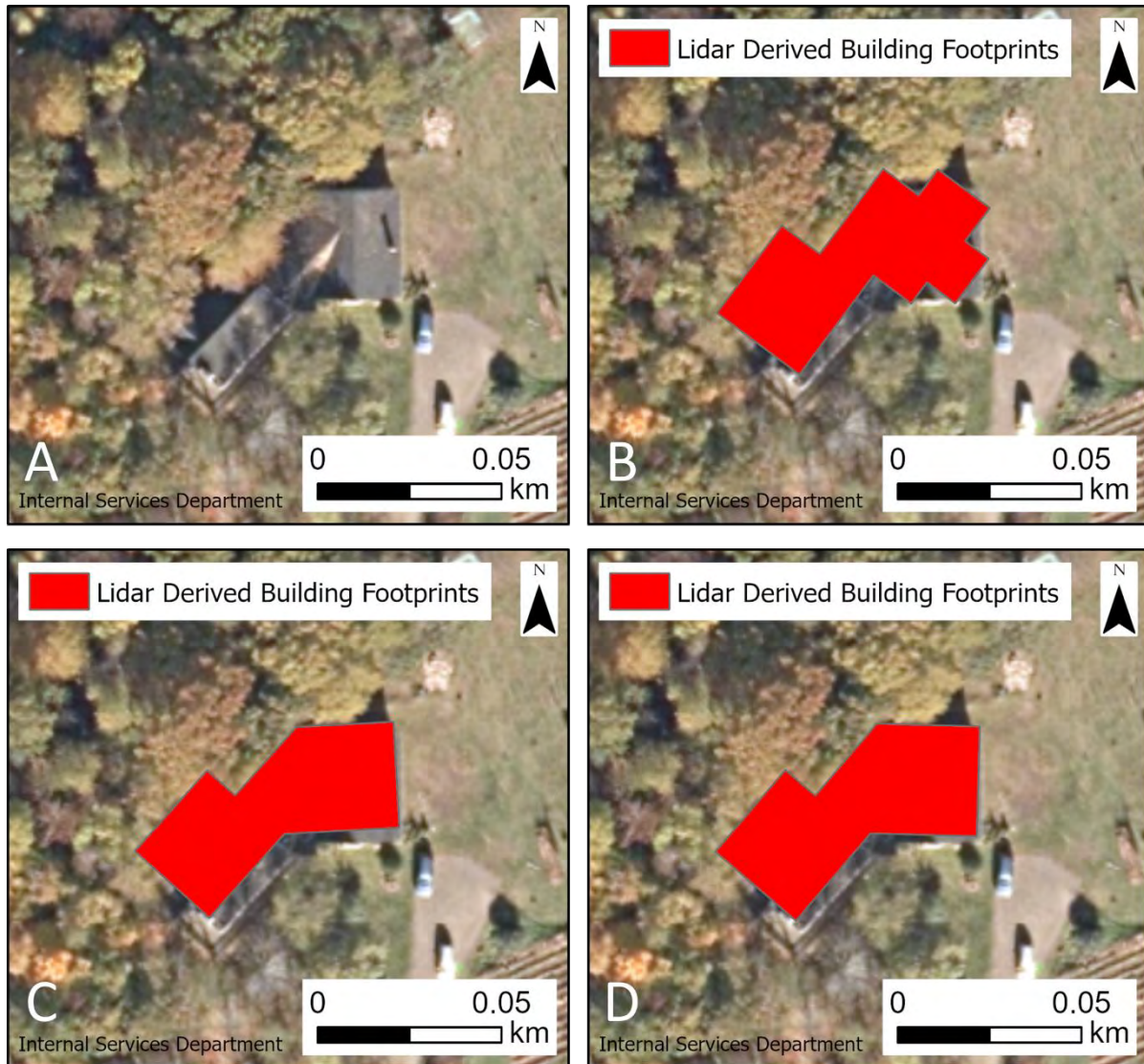


Figure 24. Maps showing a comparison between 2015 orthoimagery (A) and lidar-derived building footprints that have been regularized using right angles (B), right angles and diagonals (C), and any angle (D).



Figure 25. Maps showing a comparison between 2015 orthoimagery (A) and lidar-derived building footprints that have been regularized using right angles (B), right angles and diagonals (C), and any angle (D).

The shapes of the lidar-derived building footprints were qualitatively assessed through comparison to 2015 orthoimagery acquired by the province. Overall, the building footprints showed a good representation of the building boundaries. The lidar-derived building footprints also tended to have a greater positional accuracy and provided a less generalized building roof shape in comparison to the provincial building footprints (Figure 26).

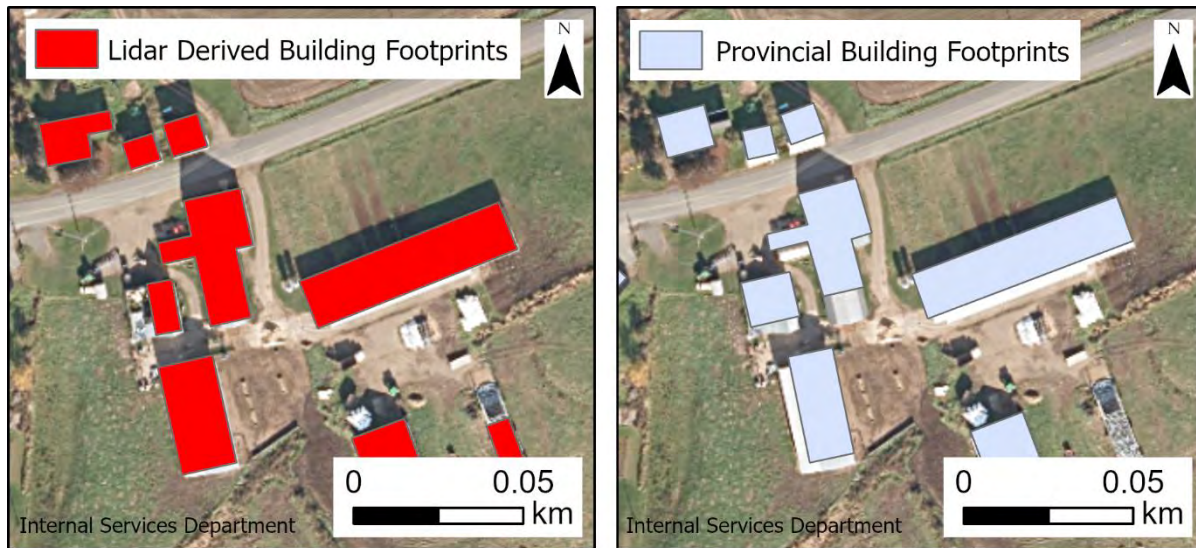


Figure 26. A side-by-side comparison of the lidar-derived and provincial building footprints.

The building footprint regularization process worked best for buildings that had a simple roof shape and were not in close proximity (<1 m) to trees. The largest contributing factor to the generation of inaccurate lidar-derived building footprints was the presence of trees that partially covered the building roof. Lidar points that belonged to buildings were either too sparse or non-existent when situated underneath dense vegetation, resulting in these irregular building shapes. Figure 27 and Figure 28 show an example of a building footprint which did not accurately represent the true shape of the building roof due to partial coverage by a tree.

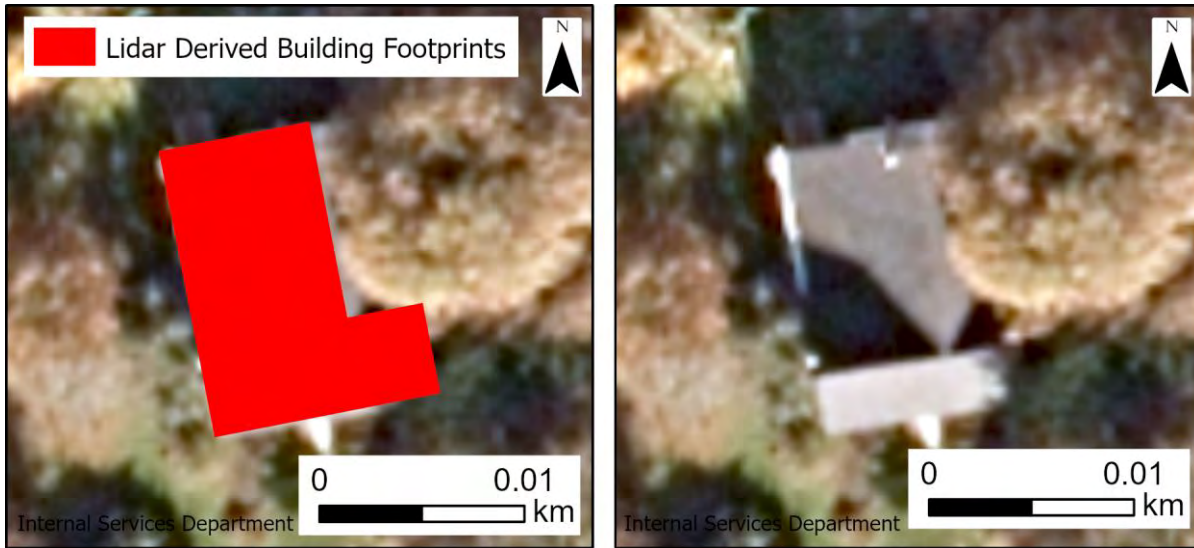


Figure 27. A comparison of a lidar-derived building footprint with 2015 provincial orthoimagery. Note the tree in the top right corner that partially covers the roof.

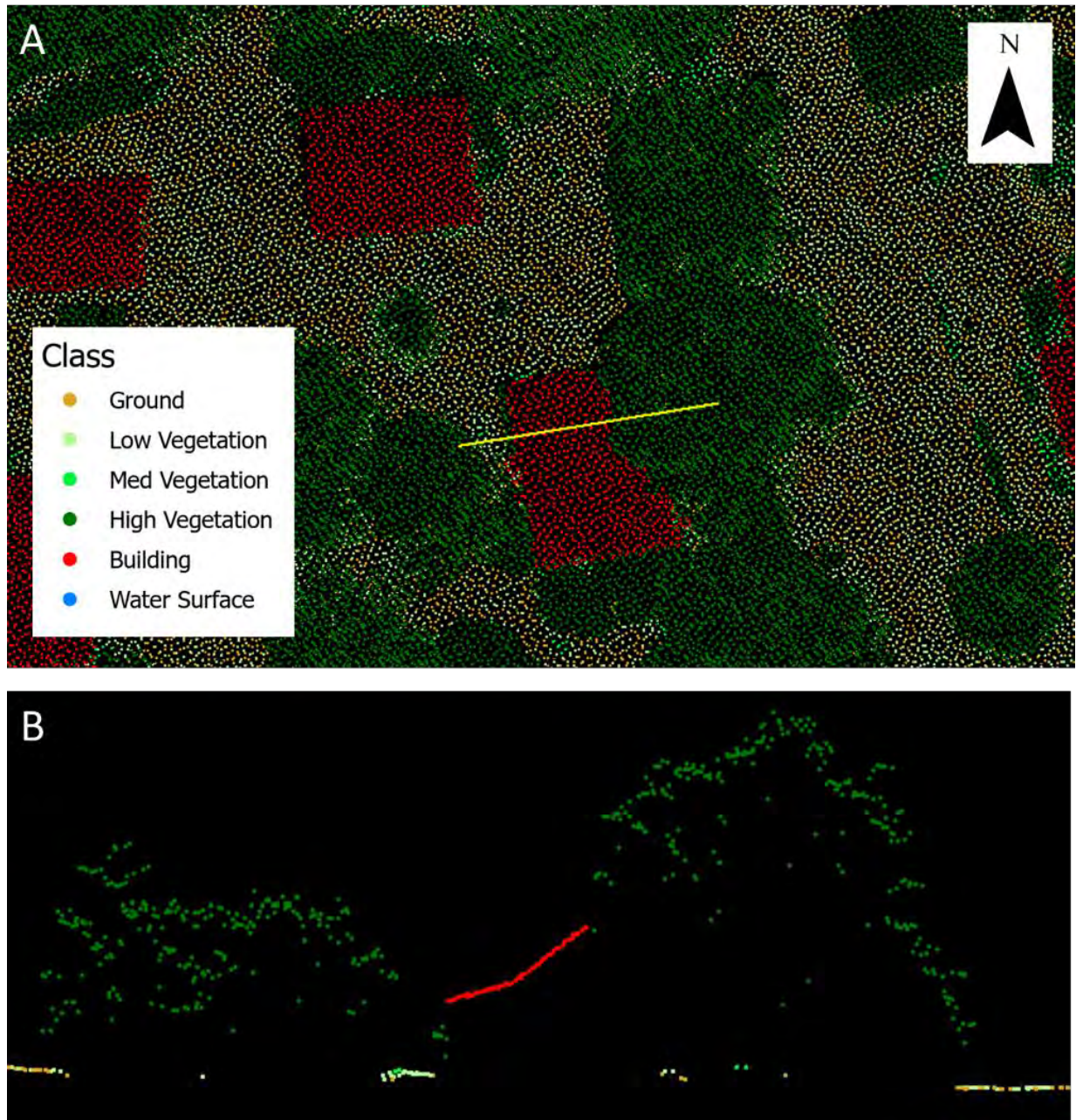


Figure 28. A cross-section of a building that is partly covered by high vegetation points. The location of the cross-section (B) is symbolized by a yellow line (A).

4.1.2.2 Expanded Assessment Area

A limitation of producing building footprints through lidar-derived methods was identified in the expanded study area, where there were buildings that were adjacent or in very close proximity (< 0.5 m) to one another. Figure 29 and Figure 30 show a cluster of buildings that have resulted in one merged footprint representing the elevation values of several buildings.

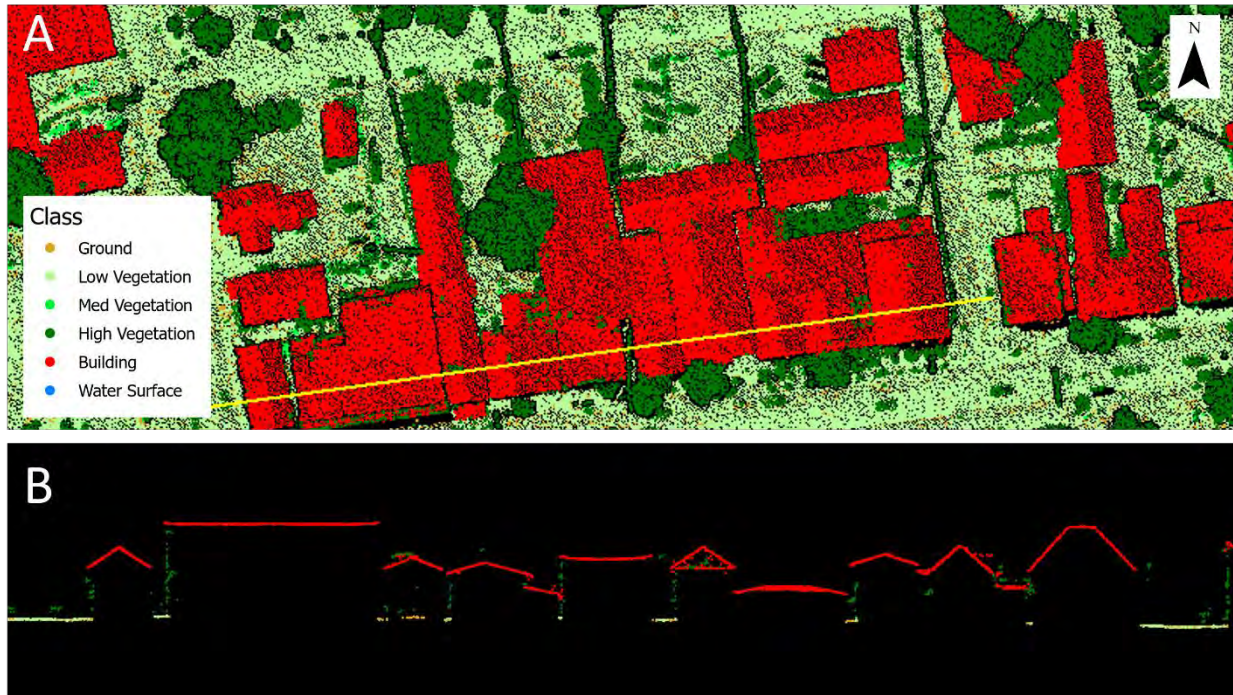


Figure 29. A cross-section of several buildings with adjacent or near-adjacent roofs. The location of the cross-section (B) is symbolized by a yellow line (A).



Figure 30. A building footprint that represents several buildings in very close proximity to one another.

4.1.3 Province-Wide Effort Estimation

The total time required to classify building points and generate building footprints with elevation information at a provincial scale was estimated to be 6,121 hours. This estimation was based upon on the time it took to process 4 LAS tiles in a relatively rural area using a Right Angle and Diagonal footprint

regularization method. In scaling up to the provincial-wide effort, processing areas without houses will be significantly quicker whereas processing urban areas will require more time and computing power. The time required for manual classification will depend on the level of accuracy desired. LAS tiles with many buildings that are in close proximity to trees and other buildings or have complex roof shapes will require manual changes to the lidar classification and building footprints.

4.2 Land Cover Classification

4.2.1 Classifier Training

It was difficult to make the distinction between tree cover types using only lidar raster products not flown in leaf-off conditions without the support of coincident orthophotos. The classifier relied heavily on the INT image for distinguishing between conifers and deciduous as the CHM only provided data on tree height which was not useful or reliable in this context. If the lidar data were collected in leaf-off conditions this task would have been more achievable. Both the CHM and INT would have generated clear differences between the two classes as conifers would have had relatively high intensity compared to the deciduous. The shape of the tree classes would also have been perceivably different in the CHM.

Further improvements could have been made to the classifier by collecting ground truth GNSS data and RGB and NIR imagery during the flight. The GNSS data would provide clear information on which areas to use for training sites with less chance for error when compared to interpreting satellite imagery to determine tree type for classification. Coincident imagery would be valuable for providing and creating temporally appropriate data products for supplementing the lidar data in classification. Such products would include a normalized difference vegetation index (NDVI), which would offer more contrast between different types of vegetation, including tree species, especially during leaf-off conditions.

4.2.2 Expanded Assessment Area

Large scale classification was investigated at the level of the entire watershed. The SVM classification process is normally scalable and developed classifiers could be applied to a larger study area. However, issues were encountered where the intensity data from the lidar were not consistent between collection dates (Figure 31). Lidar intensity values collected during the 2020 collection were recorded at a much different scale when compared to the data collected during the 2019 collection. Lidar intensity values would need to be normalized prior to using the developed SVM classifier.

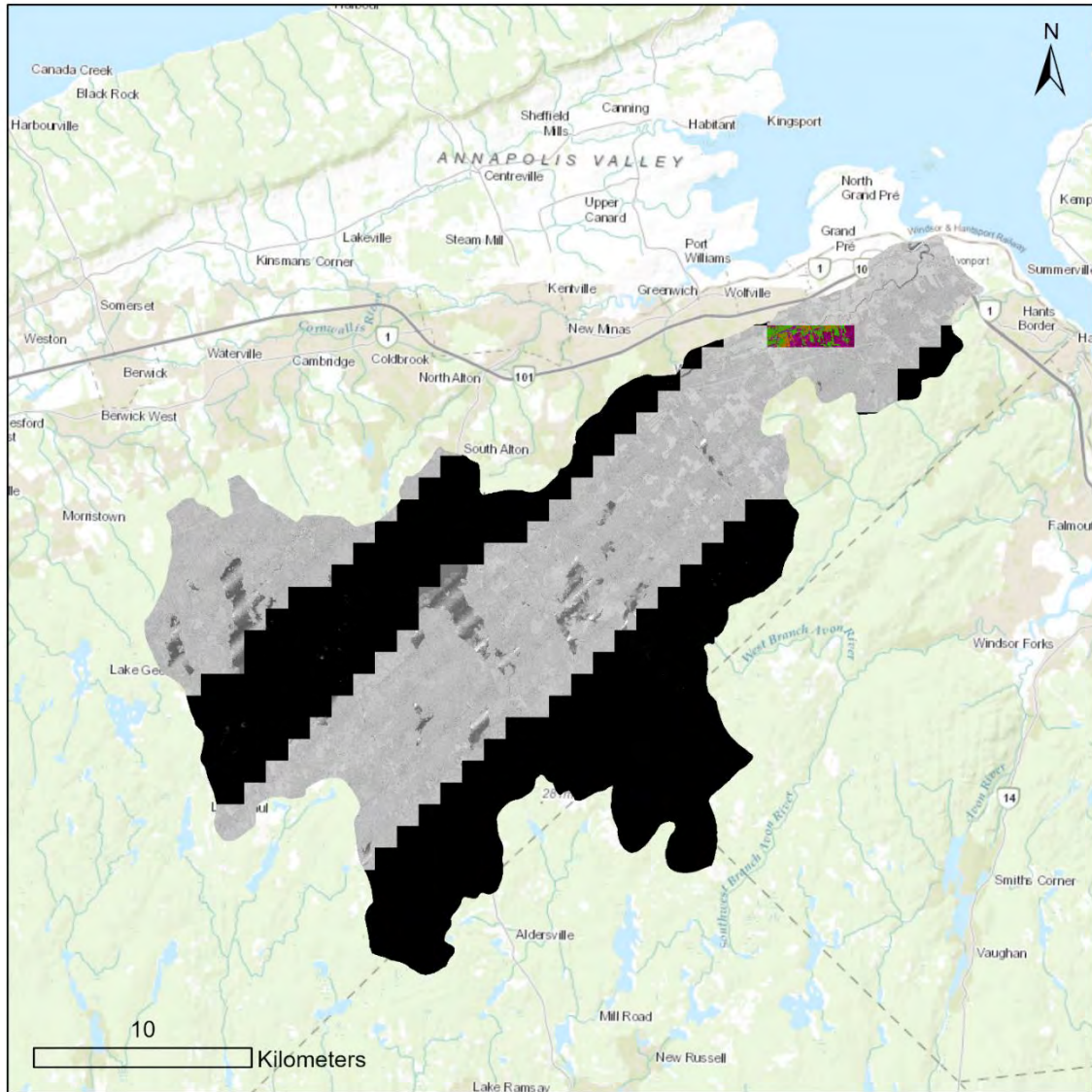


Figure 31: Overview of the full Gaspereau River – Black River watershed INT raster to demonstrate issues with the data. Classified training area overlaid for context.

4.3 Recommendations

The following section describes how information from the building and landcover classification can contribute to the understanding of the impacts of existing structures in flood risk areas.

4.3.1 Impervious Surface Layer

Classification of additional land cover classes was explored through the use of an SVM classifier on lidar-derived elevation surfaces and intensity images alongside an RGB composite orthophoto of the area. The classifier was able to identify additional impervious surfaces, such as roads and driveways, in the study

area. Roads present a hazard when they are inundated and therefore no longer safe to drive on. The province has vectors representing the location of roads, however, the impervious surface layer generated by the classifier gives a more accurate spatial representation of roads that can be paired with elevation information. AGRG was able to quantify the amount of impervious surface within the study area; this data can be used to improve hydrological modelling and better determine the level of flood risk that existing buildings within the area may experience.

4.3.2 Improved Roughness Layers for Modelling Flow

Three rasters were generated to represent the varying levels of resistance to water flow within the study area: one each for ground, low vegetation, and medium vegetation. If a more robust roughness layer were to be required, the province could follow the methodology detailed earlier for the land classification and updated lidar classification to include buildings. Friction values could then be estimated for objects that allow through-flow, such as low vegetation and trees, and over-flow, such as roads and other man-made surfaces. As described in Schubert et al. (2008), the mesh generation required for the hydrodynamic model can further be improved by adding building footprints and heights into the digital elevation model prior to mesh interpolation.

4.3.3 Improved Floodplain Prediction

Flood severity can be measured as a function of depth and velocity (FEMA, 2020). In a draft of municipal flood line mapping recommendations for Nova Scotia, depth of water and velocity were used to categorize flood hazards into three classes based on level of danger. It was recommended that this classification scheme be used to generate maps to provide municipalities with a clear visualization of the areas that are most susceptible to flood risk and be used to inform future development (Department of Municipal Affairs and Housing, 2022). With municipalities relying on these maps to inform them of flood risk areas, it is critical that the data behind the predictions be as informative as possible.

As an example of how to improve the Nova Scotia predictions, the results of the lidar-derived building footprint generation could be used in conjunction with flood severity rasters to create a more accurate assessment of how many buildings exist within each flood severity category as well as detailing their size and height. This assessment would be more accurate than what is achievable now using the current repository of provincial footprints. Another product of this project, a DEM containing elevation information from both the ground and buildings, could be used to generate more robust hydraulic models, used not only to assess the full impact of flooding on development but also the impact of development on local watercourses.

5 Conclusion

The results of this project demonstrate how the classification of lidar obtained by the Province of Nova Scotia can be updated to include buildings and that classified points can then subsequently be used to generate building footprints that contain ancillary elevation metrics. A comparison of the lidar-derived and provincial building footprints revealed that the province's database is incomplete. Extending this classification effort province-wide would result in more current data describing the location and elevation of buildings, which could be used to identify the number of buildings situated within a floodplain and their level of risk based on different degrees of inundation. Hydrodynamic models that include building footprints in their development will be more accurate as buildings greatly affect the flow of water.

The lidar classification was negatively impacted by insufficient point density, partial or complete occlusion, and building size. Additional limitations included steep roof shapes, greenhouses, inaccurate ground classification, and dense vegetation with a uniform height. Separate building footprints were observed to merge as a result of the resolution of the building elevation grid (0.5 m). Constructing higher resolution grids would somewhat alleviate this issue, however, this option would increase the overall time and computational effort required to generate building footprints. Manual classification and polygon editing are recommended to fix errors generated by the automated process.

Floodplains tend to be characterized by the presence of grasses and shrubs, as development is not common in these at-risk regions. It is important to note that the accuracy of roughness coefficients for such areas is somewhat limited because it is difficult for lidar to penetrate through very dense vegetation and reach the ground. For example, Webster, Crowell & Kodavati (2020) observed a difference of approximately 30 cm when comparing the ground elevation recorded by a topo-bathymetric lidar sensor alongside the associated GNSS validation points. It is important that data providers produce a realistic accuracy assessment of the lidar collected in floodplains to enable a better estimate of topography under dense vegetation, ultimately improving flood risk assessment.

When using lidar data to generate roughness layers, the accuracy of floodplain data is not the only concern. Cross-sections of river depth are not a requirement for airborne lidar accuracy assessments when collected at a low water level. There is no clear requirement on how to substantiate low water or that water levels were low during data collection and this lack of validation can degrade the quality of the river course data derived from the lidar. It is recommended that data providers produce metadata on river depth

or water surface elevation recorded by the lidar with tide gauge or in situ elevation data to improve the information on water flow within the region.

The outputs of this project were used to make recommendations on how to improve the Statement of Provincial Interest on Flood Risk Areas, including the need for accurate GIS layers such as an improved impervious surface layer, roughness for flow, and floodplain prediction using water depth and velocity.

The province has undergone significant changes in development since the 1980s, therefore, an up-to-date record of building locations and elevations can help to identify areas that are at significant risk for damage to lives and property. In addition, the generation of hydrologically corrected DEMs and classification of buildings and other impervious surfaces will help to generate better hydrodynamic models and subsequently help to refine the boundary between floodway and floodway fringe regions, allowing the province to establish more informed development guidelines.

6 References

- Department of Municipal Affairs and Housing. (2022). DRAFT Nova Scotia Municipal Flood Line Mapping. *Government of Nova Scotia*, 84p.
- FEMA. (2020). *Guidance for Flood Risk Analysis and Mapping: Flood Depth and Analysis Rasters*. Retrieved from https://www.fema.gov/sites/default/files/documents/fema_flood-depth-and-analysis-guidance.pdf
- Feng, B., Zhang, Y., & Bourke, R. (2021). Urbanization impacts on flood risks based on urban growth data and coupled flood models. *Natural Hazards*, 106, 613-627.
- Government of Nova Scotia. (1998). *Municipal Government Act: Statements of Provincial Interest*. Retrieved from Government of Nova Scotia.
- McGuigan, K., Webster, T., & Collins, K. (2015). A Flood Risk Assessment of the LaHave River Watershed, Canada Using GIS Techniques and an Unstructured Grid Combined River-Coastal Hydrodynamic Model. *Journal of Marine Science and Engineering*, 3, 1093-1116.
- Millward, H., Ouellette, B., & Ricketts, P. (1985). The Gaspereau Valley of Kings County, Nova Scotia: A map folio with text. (S. M. Department of Geography, Ed.) *Atlantic Region Geographical Studies*, 4, 37p.
- Province of Nova Scotia. (2017, December 10). *What is a Flood?* Retrieved from Government of Nova Scotia: <https://novascotia.ca/nse/climate-change/nsfaf-flooding.asp>
- Province of Nova Scotia. (2020). *Minimum Planning Requirements in Nova Scotia: Guidebook on Implementing the "Statements of Provincial Interest"*. Retrieved from <https://beta.novascotia.ca/sites/default/files/documents/1-2652/minimum-planning-requirements-guidebook-implementing-statements-provincial-interest-en.pdf>
- Schubert, J., Sanders, B., Smith, M., & Wright, N. (2008). Unstructured mesh generation and landcover-based resistance for hydrodynamic modeling of urban flooding. *Advances in Water Resources*, 31, 1603-1621.
- Thapa, A., Bradford, L., Strickert, G., Yu, X., Johnston, A., & Watson-Daniels, K. (2019). "Garbage in, Garbage Out" Does Not Hold True for Indigenous Community Flood Extent Modeling in the Prairie Pothole Region. *Water*, 11(2486), 18p.
- Webster, T., Crowell, N., & Kodavati, D. (2020). Topo-bathymetric survey for Hydrodynamic Modeling - River John. *Technical Report submitted to GeoNova and NS Department of Municipal Affairs*, 37p.

7 Acknowledgements

We would like to thank Colin MacDonald of Internal Services for overseeing this research agreement between the Province of Nova Scotia and NSCC.

8 Appendix

The following section includes the Terrascan macro steps used to classify buildings in raw lidar data within the study area.

```
# Move high vegetation points <=2 m above ground to a temporary class
FnScanClassifyHgtGrd(2,100.0,5,224,0.000,2.000,0)

# Classify buildings
FnScanClassifyBuilding(2,5,6,1,40.0,0.09,1,0)

# Classify high vegetation points close to buildings that have an "only echo" echo type
FnScanClassifyEcho(5,225,0,0)

FnScanClassifyCloseby("225","0-65535","0-255",6,3,0.800,0,0,1,"6",0,"0-65535",0,"0-255",0)
FnScanClassifyCloseby("225","0-65535","0-255",6,32,0.700,0,0,1,"6",0,"0-65535",0,"0-255",0)
FnScanClassifyCloseby("225","0-65535","0-255",6,31,0.500,0,0,1,"6",0,"0-65535",0,"0-255",0)

# Move temporary classes back to high vegetation
FnScanClassifyClass("224",5,0)
FnScanClassifyClass("225",5,0)
```